ACS Pharmacology & Translational Science

pubs.acs.org/ptsci

Review

Antibiofilm Peptides: Relevant Preclinical Animal Infection Models and Translational Potential

Gislaine G. O. S. Silveira, Marcelo D. T. Torres, Camila F. A. Ribeiro, Beatriz T. Meneguetti, Cristiano M. E. Carvalho, Cesar de la Fuente-Nunez, Octávio L. Franco,* and Marlon H. Cardoso*

Cite This: *ACS Pharmacol. Transl. Sci.* 2021, 4, 55−73

Read Online

ACCESS | Metrics & More | Article Recommendations

ABSTRACT: Biofilm-forming bacteria may be 10−1000 times more resistant to antibiotics than planktonic bacteria and represent about 75% of bacterial infections in humans. Antibiofilm treatments are scarce, and no effective therapies have been reported so far. In this context, antibiofilm peptides (ABPs) represent an exciting class of agents with potent activity against biofilms both *in vitro* and *in vivo*. Moreover, murine models of bacterial biofilm infections have been used to evaluate the *in vivo* effectiveness of ABPs. Therefore, here we highlight the translational potential of ABPs and provide an overview of the different clinically relevant murine models to assess ABP efficacy, including wound, foreign body, chronic lung, and oral models of infection. We discuss key challenges to translate ABPs to the clinic and the pros and cons of the existing murine biofilm models for reliable assessment of the efficacy of ABPs.

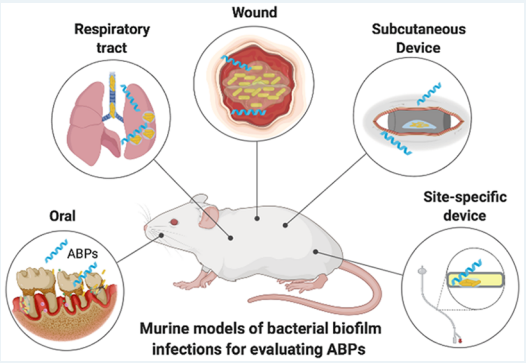

KEYWORDS: *biofilm infections, antibiofilm peptides, murine models*

INTRODUCTION

Biofilms are aggregates of microorganisms in which cells are frequently embedded in a self-produced matrix of extracellular polymeric substances (EPS) that adhere to each other and/or a surface.[1] Biofilm formation leads to increased resistance of the aggregate inhabitants to abrupt environmental changes, allowing them to live under hostile conditions.[2] Consequently, biofilm-forming bacteria may be 10−1000 times more resistant to antibiotics than planktonic bacteria and represent about 75% of bacterial infections in humans.[3] This resistance may be boosted by several genetic and phenotypic factors, including administration of antibiotics at sublethal doses, horizontal resistance gene transfer, and EPS production.[4,5]

Although many studies have focused on biofilms, there are still no antibiotics exclusively developed for this type of infection.[6] Antibiotics routinely used for the treatment of planktonic bacterial infections are also applied against bacterial biofilms, often leading to antibiofilm therapy failure, as biofilms may be more tolerant to traditional antibiotic therapy.[7] Moreover, biofilm cells can become recalcitrant, which hinders their eradication and treatment effectiveness.[7] Therefore, new approaches for biofilm treatment, including organic acids, bacteriophages, and photoinactivation, have been extensively studied.[8] Moreover, antimicrobial peptides (AMPs) are promising alternatives for the treatment of biofilm infections.[9−11]

Here, we will use the term antibiofilm peptides (ABPs) for all AMPs that are active against bacterial biofilms.[12] ABPs of either natural or synthetic origin present amphipathic and cationic characteristics and sequences of less than 50 amino acid residues. Moreover, apart from preventing biofilm formation, ABPs have been shown to eradicate preformed biofilms.[12,13] It is also worth noting that some ABPs' activity is orthogonal versus biofilms, meaning that they are not active against bacteria in their planktonic mode of growth. The mechanisms of action of ABPs have been divided into different groups.[14] The most well-known mechanisms of action include triggering changes in the bacterial membrane potential and membrane rupture.[15] ABPs can also block cell signaling and communication by interfering with biofilm-related gene expression.[16] The degradation of the biofilm polysaccharide matrix has also been reported as one of the mechanisms by which ABPs act on biofilms.[17] Moreover, ABPs have been shown to interfere with the stress response.[18]

Diverse systems have been adopted to evaluate the antibiofilm activities of different compounds *in vitro*, as extensively reviewed by Coenye and Nelis (2010).[19] Although numerous studies have evaluated ABPs *in vitro* (*e.g.*, microtiter plate-based and flow displacement biofilm), only a few have reported *in vivo* strategies for studying biofilms. Given the relevance of bacterial biofilm

Received: November 11, 2020
Published: January 27, 2021

infections worldwide, here we highlight the translational potential of ABPs and provide an overview of the different clinically relevant mouse models available to assess efficacy. This review is divided by mouse models for accessing ABPs antibiofilm activity, thus favoring the comparison of lead peptide candidates for each model and pinpointing methodological differences for a given animal model and how it can interfere with ABP activities. Therefore, for all subtopics, we provide a brief description of each model for evaluating ABPs followed by a detailed description of the positive and negative outcomes obtained for this class of antibiofilm agents.

Wound Models. Skin wound models are among the most commonly used strategies to evaluate antibiofilm compounds (Table 1). There are two approaches used for the formation of biofilms in murine skin wounds.[20] The first strategy involves causing skin damage (*e.g.*, scarification/abrasions, pressure-induced ischemic, surgical excision, or burns) and, subsequently, infecting the injured region with biofilm-forming bacteria.[21] The second strategy inoculates high-density biofilm-forming bacteria subcutaneously, leading to the formation of abscesses and wounds.[22] The main clinically relevant bacterial strains used individually or in consortium in both approaches are *Staphylococcus aureus*, *Staphylococcus epidermidis*, and *Pseudomonas aeruginosa*.[23,24]

The bacterial inoculum can vary according to the expected infection severity (Tables 1 and 2), ranging from acute to chronic. The latter mimics biofilm infections in humans most accurately.[25] Antibiofilm activity is evaluated by bacterial recovery from the infected wound. The infection site is excised, macerated, and serially diluted to determine the number of biofilm-forming bacteria, expressed as colony-forming units (CFU) per gram (CFU g^{-1}) of tissue.[26] Nevertheless, other approaches have also been used to evaluate ABP effectiveness (Table 1 and 2), including (i) analyses of the infectious process and healing through real-time imaging with an *in vivo* imaging system (IVIS), along with wound size measurement with the aid of calipers and photographs;[23,27] (ii) histological analysis (*e.g.*, hematoxylin eosin) and histochemistry to evaluate the tissue regeneration process; (iii) analysis of genetic signatures associated with biofilm formation (*e.g.*, *pslD*, *mucC*, and quorum sensing (QS) related genes); (iv) evaluation of underlying organs (*e.g.*, liver, lung, kidneys); and (v) evaluation of inflammatory patterns (*e.g.*, IL-6, IL-10, and TNF-α) (Figure 1).[21,23,26,27]

Torres et al. (2018)[28] reported a skin scarification mouse model to establish a *P. aeruginosa* abscess on mice dorsum to evaluate the anti-infective potential of short AMPs. The authors did not immunosuppress the mice and focused on evaluating bacterial load exclusively by applying a single superficial treatment. After 2 or 4 days, the wounded skin was excised, and CFU counts were used to evaluate the peptides' anti-infective effect. Similar studies were conducted for computationally designed peptides (Table 2).[29−32] More recently, a peptide named RP557 (Table 2) was shown to effectively eliminate biofilms in a murine abrasion model infected with methicillin-resistant *S. aureus* (MRSA). Only a 0.2% topical dose of RP557 was required to eliminate MRSA biofilms. Moreover, MRSA demonstrated low resistance to RP557 after several passages with sublethal concentrations.[27]

Considering the importance of QS for bacterial biofilms, Nakagami et al. (2008)[21] reported a pressure-induced ischemic wound rat model using *P. aeruginosa*. The authors demonstrated the presence of QS molecules in the infected wounds and showed QS's role in *P. aeruginosa* biofilm wound infections. Later, Schierle et al. (2009)[33] developed a new cutaneous excision model infected with *S. aureus* and *S. epidermidis* biofilms, in which QS inducers were observed and related to *Staphylococcal* biofilm formation, leading to skin re-epithelialization and healing delay during the infection process. By contrast, *S. aureus* or *S. epidermidis*-infected wounds treated with RNAIII-inhibiting peptide (RIP) (Table 2) showed accelerated wound healing.[33]

In terms of polymicrobial biofilm infections, Chung et al. (2017)[23] demonstrated the *in vivo* antibiofilm activity of DRGN-1 (Table 2), a peptide designed from the peptide VK25. The polymicrobial biofilm was grown in a polycarbonate filter and implanted over an incision made on the mouse dorsum. DRGN-1 was administrated topically and reduced the microbial load (2-log) at the infection site. It also induced keratinocyte migration to the injured region, substantially improving the healing process.[23]

Burn wounds can be colonized by a biofilm, aggravating healing. Ma et al. (2017)[26] evaluated WRL3 (Table 2), a peptide that synergized with ceftriaxone against MRSA biofilms *in vivo* using a scald-burn wound model. This peptide demonstrated potent activity, inhibiting biofilm growth, reducing biofilm biomass, and promoting wound healing.[26]

Biofilm infections in wound sites are challenging to treat and usually lead to cutaneous abscess formation. Mansour et al. (2016)[34] used a mouse model to evaluate ABPs' activity against MRSA cutaneous abscesses. The peptide DJK-5 (Table 2) was investigated in systemic (6 or 4 mg kg^{-1}) and cutaneous (3 or 4 mg kg^{-1}) models for MRSA and *P. aeruginosa*. When administrated topically, DJK-5 reduced skin damage and significantly decreased the local bacterial load.[34] Although DJK-5 revealed potent antibiofilm activity, studies have shown that this peptide can cause tissue damage and inflammation at 1.5 mg mL^{-1}.[35] To overcome this obstacle, Kłodzińska et al. (2019)[35] evaluated the potential of DJK-5 encapsulated within hyaluronic acid−based nanogels. Similar antibiofilm activities were reported, and the encapsulated DJK-5 system led to 4-fold decreased toxicity compared with free DJK-5.[35]

Kumar et al. (2019)[36] also used a cutaneous abscess model to evaluate the activity of aurein-derived peptides. Among the molecules evaluated, peptide 73 (Table 2) was 2.2-fold more efficient at reducing MRSA cutaneous abscesses than its parent peptide. The *in vivo* antibiofilm potential was further enhanced by incorporating cysteine residues to the C-terminus of peptide 73 and performing chirality changes or encapsulating peptide 73 in polymers (*e.g.*, polyethylene glycol (PEG) or hyperbranched polyglycerol (HPG)).[36] This cutaneous abscess model was used by Pletzer et al. (2018)[37] in a high-throughput *in vivo* study with the peptides HHC-10, IDR-1002, IDR-1018, and DJK-5 (Table 2). The synergistic activity of these peptides in combination with conventional antibiotics was investigated against ESKAPE pathogens (*Enterococcus faecium*, *S. aureus*, *Klebsiella pneumoniae*, *Acinetobacter baumannii*, *P. aeruginosa*, and *Enterobacter* species), leading to reduced abscess size independent of the mechanism of action of either antibiotics or ABPs.[37]

Most of the studies mentioned demonstrate that ABPs operate by decreasing bacterial load and triggering tissue healing processes.[21,28,31,33] Although we focused on describing studies that exclusively reported antibiofilm activity *in vivo*, such studies can be challenging. This may occur due to many factors, including bacterial load, bacteria inoculation versus treatment with APBs, and administration route. For instance, treatment with peptides is often initiated at the same time or within minutes after bacterial inoculation.[34,36] An alternative that can overcome this issue is the model proposed by Chung

https://dx.doi.org/10.1021/acsptsci.0c00191
ACS Pharmacol. Transl. Sci. 2021, 4, 55−73

Table 1. Studies Using *In Vivo* Bacterial Biofilm Infection Models to Evaluate ABPs

		murine host	bacteria	bacterial load	bacterial route	peptide	treatment route	dose effect	analysis	time exp.	results	ref
wound	skin scarification an abrasion	female CD-1 IGS mice	*P. aeruginosa* (PA14)	~10^7 CFU in 50 μL	inoculated with a pipet tip	[Lys]7-Pol-CP-NH_2	topic injection	64 μmol L^{-1} (single dose 1 day postinfection)	bacterial load and body weight	2/4 days	skin infections were sterilized 4 days after infection	28
		female CD-1 mice	*P. aeruginosa* (PAO1)	5.5 × 10^7 CFU in 20 μL	inoculated with a pipet tip	(P)PAP-A3	topic injection	50 μM in 20 μL (single dose 1 day postinfection)	bacterial load	4 days	4-log CFU reduction	30
		female CD-1 mice	*P. aeruginosa* (PA14)	5 × 10^7 CFU in 20 μL	inoculated with a pipet tip	EcDBS1R5	topic injection	64 μM (single dose 1 day postinfection)	bacterial load	2 days	2-log CFU reduction	31
		female CD-1 mice	*P. aeruginosa* (PA14)	5 × 10^6 CFU in 20 μL	inoculated with a pipet tip	PaDBS1R6F10	topic injection	64 μM (single dose 1 day postinfection)	bacterial load	2/4 days	3-log CFU reduction 4 days postinfection	32
		female BALB/c	MRSA (bioluminescent Xen31)	10^8 CFU mL^{-1} in 40 μL	inoculated with a pipet tip	RP557	topic	0.2% in 40 μL (single dose 4 h postinfection)	bioluminescence of viable cells and body weight	7 days	2-log CFU reduction 7 days postinfection; decreased body weight loss	27
		female CD-1 IGS mice	*P. aeruginosa* (PA14)	5 × 10^7 CFU in 50 μL	inoculated with a pipet tip	mastoparan-R1 and R4	topic injection	64 μM in 20 μL (single dose 1 day postinfection)	bacterial load	2/4 days	2-log CFU reduction at day 2 postinfection	29
	pressure ulcer	male SPF Wistar rats	*P. aeruginosa* (PAO1)	1.6−2.4 × 10^5 CFU mL^{-1} in 0.1 mL	intracutaneous and intramuscular injection and topical				QS autoinducer quantification (3OC12-HSL)	3/7 days	correlation between autoinducer concentration and bacterial counts was observed	21
	surgical	male C57Bl6/J mice	*S. aureus* (CFS101) *S. epidermidis* (CFS201)	preformed biofilm	applied wound	RIP	topic injection	1 mg mL^{-1} in 0.1 mL (single dose 3 days postinfection)	bacterial load, histology, and Gram's stain	9 days	sterilized skin infections post 7 days and delayed wound healing effects post 9 days	33
		female BALB/c mice	*S. aureus* (ATCC 25923) *P. aeruginosa* (ATCC 9027)	1000:1 and grown on a polycarbonate filter	preformed biofilm applied to the wound	DRGN1	topic	20 μg in 20 μL (every 2 days until the 6th day)	bacterial load, wound healing and histological	6 days	promoted the migration of keratinocytes, reduced bacterial load, and improved healing	23
	iron burn	male ICR mice	MRSA (ATCC 43300)	4 × 10^8 CFU mL^{-1} in 50 μL	inoculated into burn	WRL3	topic	4 μg mL^{-1} in 50 μL (twice a day for 14 days)	bacterial load, histological, cytokines dosage, chemotaxis	14 days	MRSA proliferation control, bacterial load reduction and healing induction	26
	cutaneous abscess	female CD-1 mice	*S. aureus* (HG001 bioluminescent)	5 × 10^7 CFU in 50 μL	injected right flank of the back	DJK-5	i.p intra-abscess	6 mg kg^{-1} in 50 μL (single dose before infection)3	bacterial load, imaging system and abscess area measure	5 days	10.2-fold CFU reduction after 5 days and reduced dermonecrosis	34
								3 mg kg^{-1} in 50 μL (single 1 h postinfection)	bacterial load, abscess area measure, histological and weight loss/gain	3 days	lesion size 4.6-fold smaller, 8.4-fold fewer bacteria, less tissue damage and weight gain	
		female CD-1 mice	*P. aeruginosa* (LESB58)	5 × 10^7 CFU in 50 μL	injected right flank of the back	DJK-5	i.p intra-abscess	4 mg kg^{-1} in 50 μL (single dose before infection)	bacterial load and abscess area measure	3 days	2.2-fold smaller abscess lesions	34
								4 mg kg^{-1} in 50 μL (single dose 2 h postinfection)		3 days	2.2-fold smaller abscess lesions and 2.7-fold smaller lesions	
		female outbred CD-1	*P. aeruginosa* (LESB58)	5 × 10^7 CFU mL^{-1} in 50 μL	injected right flank of the back	DJK-5 with hyaluronic acid−based nanogels	intra-abscess	3−6 mg mL^{-1} in 50 μL (single dose 1 h postinfection)	bacterial load and abscess lesion measure	3 days	bacterial load reduction	35

https://dx.doi.org/10.1021/acsptsci.0c00191
ACS Pharmacol. Transl. Sci. 2021, 4, 55−73

Table 1. continued

		murine host	bacteria	bacterial load	bacterial route	peptide	treatment route	dose effect	analysis	time exp.	results	ref
		female outbred CD-1	*S. aureus* (LAC)	5×10^7 CFU mL^{-1} in 50 μL	injected right flank of the back	peptide 73 peptide 73-C micelles	intra-abscess	5 mg kg^{-1} in 50 μL (single dose 1 h postinfection)	bacterial load and abscess lesion measure	3 days	8.9-fold bacterial load reduction and 80% abscess reduction	36
		female outbred CD-1	*P. aeruginosa* (LESB58) *A. baumannii* (Ab5075) *E. faecium* *K. pneumoniae* (KPLN649) *E. coli* (E38) *S. aureus* (LAC)	5×10^7–2×10^{10} CFU mL^{-1} in 100 μL	injected right flank of the back	DJK5 HHC-10 IDR-1002 IDR-1018	intra-abscess	(3, 0,25 and 10 mg kg^{-1} in 100 μL (single dose 1 h postinfection)	bacterial load and abscess lesion measure	3 days	bacterial load reduction and abscess sizes; improved activities in synergism with antibiotics	37
	urinary tract stents	female Wistar rat	*S. aureus* Smith diffuse (SD)	2×10^7 CFU mL^{-1}	injected into the bladder	RIP	stents impregnated with RIP	1 μg mL^{-1} 30 min immediately before implantation	bacterial load of stent and urine	5 days	2-log CFU reduction in stent and urine	43
foreign body site specific devices	central venous catheters	male Wistar rat	*S. aureus* (SD)	1×10^6 CFU in 0.1 mL	injected into CVC after 30 min treatment	citropin 1.1 BMAP-28	via CVC	before infection, single dose 10 μg mL^{-1} in 0.1 mL	bacterial load of peripheral blood and catheters/venous tissues	24 and 9 days	Reduced CFU counts in peripheral blood cultures and CVC and synergy with antibiotics bacteremia was eliminated 4-log CFU mL^{-1} reduction and bacteremia in monotherapy and synergy with antibiotics decreased to 6-log and bacteremia was not detected	42 46
			E. faecalis S.aureus (SD)			IB-367					bacterial load in biofilms was decreased; bacteremia was not detected during synergistic treatment with antibiotics	47
	periprosthetic joint	female B57BL/6 J mice Jackson	*S. aureus* (SH1000)	10 μL with 1×10^6 CFU	injected joint space	WLBU2	i.p.	0.01 mg kg^{-1} and 10 mg kg^{-1} 24 h after and twice a day for 3 days	biofilm mass of implant and femur homogenate	3 days	decreased biofilm mass of implant and tissue	49
	urethral stent	male Wistar rat	*P. aeruginosa* (ATCC 27853)	(1 mL) containing 2×10^7 CFU mL^{-1}	injected graft surface	tachyplesin III	ureteral stent	10 mg L^{-1} Coated implanted	bacterial load of stent	5 days	3-log CFU reduction in monotherapy and 5-log reduction in synergy with antibiotics	50
foreign body subcutaneous devices	catheter needle	BALB/c nude mouse	*P. aeruginosa* (3241)	5×10^8 CFU mL^{-1}	preformed biofilm on a catheter needle 24 h	HPA3NT3-A2	catheter	50 μg mL^{-1} added to the biofilm formed into catheter	histological analyses skin, spleen, and kidney	7 days	less epidermis, dermis, or hypodermis damage at the implantation site	54
		BALB/c mice	*P. aeruginosa* (MDR)	1×10^8 CFU mL^{-1}	preformed biofilm on a catheter 24 h	EC1-17KV	at the implant site	10 mg kg^{-1} once daily for three continuous days	bacterial load and pathological examination	3 days	3.5- and 2.7-log unit CFU reductions in the subcutaneous tissue and catheter surface, respectively, and protective	53

https://dx.doi.org/10.1021/acsptsci.0c00191
ACS Pharmacol. Transl. Sci. 2021, 4, 55−73

Table 1. continued

		murine host	bacteria	bacterial load	bacterial route	peptide	treatment route	dose effect	analysis	time exp.	results	ref
											effect against the inflammatory injury	
		female C57BL/6 mice	*S. aureus* (USA300 LAC)	20 μL with 10^3 CFU/catheter	injected into the lumen of the catheter	17tF-W	catheter lumen	250 μg 2, 24, and 48 h postinfection, 50 μL per site	bacterial load of tissue and catheter/chemokine levels	3 days	eliminated the burden in both mouse-embedded catheters and their surrounding tissues, suppressed the level of chemokine TNFα, and boosted chemokines MCP-1, IL-17A and IL-10	55
	titanium coating	female SPF BALB/c mice and Sprague–Dawley rat	*S. aureus*	100 μL of 10^7 and 10^5 CFU per site	injected into site biomaterial bed	cys-melimine	titanium coating	built into the titanium disc inserted in the back of the animals	bacterial load	5 and 7 days	bacterial load reduction in both models	51
	Dacron grafts	male Wistar rat	MRSA and MRSE	2×10^7 CFU mL^{-1}	injected into the graft surface	DD_{13}-RIP	peptide binding to Dacron	50 μg mL^{-1} for 0.5 and 5 h	bacterial load	7 days	bacterial load reduction of staphylococcal associated with graft at the lowest dose	56
	silicone implants	male SPF BALB/c	*P. aeruginosa* (PAO1)	initial concentration of OD600 = 0.1 in LB medium	preformed biofilm into 4 mm silicone tubes for 12h	melittin	injected at the incision site	50 mg kg^{-1} after 1 day of incision	bacterial load, tissue damage and biofilm colonization	3 days	bacterial load reduction and prevented tissue damage and inflammation in synergy with antibiotics	52
	silicone sheets	female BALB/c	*P. aeruginosa* (ATCC 15442)	1 mL of 10^5 CFU mL^{-1}	preformed biofilm into PDMS sheets (0.2 × 0.6 cm^2) for 48 h	CS-PEG-LK_{13}	injected in situ	6.7 mg kg^{-1} once a day after 24 h surgery	bacterial load and pathology of the tissue.	4 days	improved healing, eradication of biofilm, tissues (muscle and skin) reduced inflammation and production of IL-6 and TNF-α	57
	alginate	female Lewis rats	*P. aeruginosa* (NH57388A)	10^{10} CFU mL^{-1}	intratracheal instillation	Novispirin G10	instillation into the lower left lung	0.1 mg mL^{-1} in 0.1 mL	bacterial load in the lung pathology and histology and cytokines	3, 5, 7, and 10 days	bacterial load reduction of the lung, inflammatory cytokines, and a decrease in inflammation	63
	agar bead coated	rats	*P. aeruginosa mucoid* (PAO1)	10^4 CFU mL^{-1}	preformed biofilm agar beads intratracheally	HBCM2, HBCM3, HBCPα-2 and HB71	intratracheally instillation or nebulization	100 g in 100 μL 3 days after inoculation once daily or 5 mg mL^{-1} once daily for 3 days	bacterial load in the lung	3 days	bacterial load reduction in the lung	60
respiratory		female BALB/c	*P. aeruginosa* (PAO1)	8×10^6 UFC in 20 μL	intranasally	P5 and P6.2	intranasally	10 mg kg^{-1} 30 minutes after infection.	bacterial load and cytokines in the lung	20 h	bacterial load reduction in the lung and decrease in pro-inflammatory cytokines	65
	bacterial solution	female C57BL/6	*P. aeruginosa* (C1)	1×10^6 CFU in 40 μL	intranasally	ZY4	intravenously	2, 4, and 8 mg kg^{-1}, 1 h postbacteria inoculation twice a day for 3 days	bacterial load in the lung, blood cytokines and lung histopathology	72 h	bacterial load reduction of 90% of the lung, alleviated lung inflammation, reduced infiltration of inflammatory cells and up-regulation of cytokine levels (IL-6, TNF-α, IL-1β, and IL-10)	66

https://dx.doi.org/10.1021/acsptsci.0c00191
ACS Pharmacol. Transl. Sci. 2021, 4, 55−73

Table 1. continued

		murine host	bacteria	bacterial load	bacterial route	peptide	treatment route	dose effect	analysis	time exp.	results	ref
		female wild-type C57BL/6J	*P. aeruginosa* (PAO1)	~3 × 10^6 CFU per mouse in 50 μL	intratracheally	Esc (1−21), Esc (1−21)-1c, LL-37	intratracheally	0.1 mg kg^{-1} 2 and 12 h after	bacterial load, cytokines and airway-epithelia associated genes	24 h	bacterial load reduction of lung, reduced leukocyte recruitment, and attenuated inflammatory response	67
		female wild-type C57BL/6J	*P. aeruginosa* (PAO1)	~3 × 10^6 CFU in 50 μL	intratracheally	WLBU2 WLBU2- D8	ontratracheally	0.05 mg kg^{1-} in 50 μL 1 h after infection	bacterial load and histopathology of the lungs		bacterial load reduction in the lung and reduced inflammatory response; bacterial load reduction in the lung and reduced inflammatory response; therapeutic index greater than 140	68
		C57BL/6J mice	*K. pneumoniae*	1 × 10^5 CFU	intranasal instillation	IK8L	vein injection	20 mg kg^{1-} 4 h before infection	bacterial load, survival, biophotonic imaging, cytokines and lung histopathology	50 h	bacterial load reduction in the lung, reduced lung injury, longer survival, TNF-α, IL-6, and IL-1β decrease	72
oral	dental caries	weaned Sprague−Dawley rats	*S. mutans* (UA159)	mid logarithmic culture	oral (every day for 5 days)[a,b]	LN-7	topic on the molars	32 μM, twice a day for 6 weeks	Caries scores by Keyes system and macroscopic tissue lesions	72 days	slight dentinal lesions in the sulcal surface reducing the occurrence of severe dental lesion	78
		weaned Sprague−Dawley rats	*S. mutans* (UA159)	mid logarithmic culture	orally (once a day)[a,b]	GH12	topic on the molars	8 mg L^{-1} three times a day for 3 weeks	Caries scores by Keyes system, mucosal tissues histopathology and bacterial load by qPCR of saliva and scraped plaque.	21 days	lower score for both smooth-surface and sulcal-surface lesions	82
	periodontitis	BALB/cByJ mice	*S. gordonii* (DL-1) and *P. gingivalis* (ATCC 33277)	10^9−10^7 CFU in 1 mL of 2% carboxymethylcellulose	orally (five times in total, every 2 days)[a]	BAR	orally	3.4 μM every 2 days for 5 days together with *P. gingivalis*[c]	bacterial load by PCR of oral cavity and alveolar bone loss	80 days	inhibition of *P. gingivalis S. gordonii* biofilms interaction, reduced alveolar bone loss	85
		BALB/cByJ mice	*S. gordonii* (DL-1) and *P. gingivalis* (ATCC 33277)	10^9−10^7 CFU in 1 mL of 2% carboxymethylcellulose	orally (five times in total, every 2 days)[a]	BAR	orally	0.7 μM or 3.4 μM every 2 days for 5 days together with *P. gingivalis*[c]	bacterial load, alveolar bone loss, and maxillary molar histology	80 days	biofilm formation and periodontitis inhibition, reduced inflammatory process, and lower alveolar bone loss	89
		male Sprague−Dawley	*P. gingivalis* (W83)	1 × 10^9 CFU mL^{-1} in 1.5 mL	orally (twice times every day for 4 weeks)[d]	Nal-P-113	topic into periodontal pockets	6.25, 25, 100, or 400 μg mL 2 h later infection twice times every day for 4 weeks	alveolar bone loss, bacterial colonization, and distribution by scanning electron microscopy and qPCR; histopathologic of periodontal tissue and Western blot detection of gingival tissue	45 days	alveolar bone loss inhibition; decreased bacterial load in biofilms; IL-1β and TNF-α decreased in the periodontal tissue	92

[a]Previous treatment with antibiotics to deplete the oral microbiome. [b]Offered cariogenic diet *ad libitum* throughout the experiment. [c]Observation for 47 days and then euthanasia. [d]Placement of a ligature around the first molars from the rats before infection.

https://dx.doi.org/10.1021/acsptsci.0c00191
ACS Pharmacol. Transl. Sci. 2021, 4, 55−73

Table 2. ABP Sequences, Physicochemical Properties, and *In Vivo* Potential[a]

peptide name	sequence	a.a.[b]	MW[c]	pI[d]	net charge	H (%)[e]	μH[f]	*in vivo* potential	ref
[Lys]7-Pol-CP-NH_2	ILGTILKLLKSL-NH_2	12	1311.71	10.00	2	80.2	0.764		28
(P)PAP-A3	PIMYKVPLIRKKSLRRTLSERGLLKDFLKKHNLNPARKYFPQWKAPTL	48	5792.03	11.17	11	34.1	0.122		30
EcDBS1R5	PMKKLKLALRLAAKIAPVW	19	2147.78	11.33	5	57.9	0.413	skin scarification an abrasion	31
PaDBS1R6F10	KKLRLKIAFK	10	1244.63	11.33	5	23.3	0.021		32
RP557	RFCWKVCYKGICFKKCK	17	2140.71	9.62	6	58.9	0.060		27
mastoparan-R1	KILKRLAAKIKKIL	14	1636.19	11.39	6	36.9	0.775		29
mastoparan-R4	INLKKLAARIKKKI	14	1637.13	11.39	6	20.4	0.472		
RIP	YSPWTNF-NH_2	7	913.98	5.52	n.d.	n.d.	n.d.	surgical urinary tract stents	33, 43
DRGN1	PSKKTKPVKPKKVA	14	1535.94	10.70	6	−5.8	0.013	surgical	23
WRL3	WLRAFRRLVRRLARGLRR-NH_2	18	2351.88	12.85	8	25.6	0.838	iron burn	26
DJK-5	vqwrairvrvir-NH_2	12	1551.90	12.48	4	46.3	0.267		34, 35, 37
peptide 73	RLWDIVRRWVGWL	13	1755.10	11.70	2	81.5	0.753		36
peptide 73-C	RLWDIVRRWVGWLC	14	1857.24	10.26	2	86.6	0.670	cutaneous abscess	37
HHC-10	KRWWKWIRW-NH_2	9	1444.75	12.02	4	75.6	0.672		
IDR-1002	VQRWLIVWRIRK-NH_2	12	1653.05	12.30	4	66.7	0.201		
IDR-1018	VRLIVAVRIWRR-NH_2	12	1536.93	12.48	4	62.3	0.271		
citoprin 1.1	GLFDVIKKVASVIGGL-NH_2	16	1615.98	8.59	1	62.3	0.614		42
BMAP-28	GGLRSLGRKILRAWKKYGPIIVPIIRI-NH_2	27	3074.84	12.02	7	55.7	0.522	CVC	46
IB-367	RGGLCYCRGRFCVCVGR-$CONH_2$	17	1905.31	9.37	4	53.0	0.204		47
WLBU2	RRWVRRVRRWVRRVVRVVRRWVRR	24	3398.0	13.08	13	14.1	0.789	periprosthetic joint respiratory (bacterial solution)	49, 68
tachyplesin III	KWCFRVCYRGICYRKCR-NH_2	17	2240.75	9.79	5	53.6	0.050	urethral stent	50
HPA3NT3-A2	AKRLKKLAKKIWKWK-NH_2	15	1925.48	11.47	8	15.9	0.607		54
EC1-17KV	GWWRRTVKKVRNAVRKV	17	2139.6	12.48	7	13.8	0.657	catheter needle	53
17tF-W	GX_1KRlVQRlKDWlRKLV-NH_2	17	2229.78	n.d	5	n.d.	n.d.		55
cys-melimine	CTLISWIKNKRKQRPRVSRRRRRRGGRRR	29	3733.47	12.70	15	−16.2	0.148	titanium coating	51
DD_{13}-RIP	ALWKTLLKKVLKAYSPWTNF-$CONH_2$	20	2407.93	10.18	4	62.7	0.562	Dacron grafts	56
melittin	GIGAVLKVLTTGLPALISWIKRKRQQ	26	2847.49	12.02	5	51.1	0.394	silicone implants	52
CS-PEG-LK13	LKLLKKLLKKLKK	13	1594.19	10.78	7	25.2	0.809	silicone sheets	57

https://dx.doi.org/10.1021/acsptsci.0c00191
ACS Pharmacol. Transl. Sci. 2021, 4, 55−73

Table 2. continued

peptide name	sequence	a.a.[b]	MW[c]	pI[d]	net charge	H (%)[e]	μH[f]	*in vivo* potential	ref
novispirin G10	KNLRRIIRKGIHIIKKYG	18	2206.76	11.75	7	23.3	0.645	respiratory (alginate)	63
HBCM2	KWKSFIKKLTKAAKKVVTTAKKPLIV-NH_2	26	2955.75	10.90	9	31.5	0.491	respiratory (agar bead coated)	60
HBCM3	KWKKFIKSLTKSAAKTVVKTAKKPLIV-NH_2	27	3042.83	10.90	9	30.1	0.394		
HBCPα-2	KWKKFIKKIGIGAVLKVLTTGLPALKLTKK-NH_2	30	3322.26	10.90	9	45.3	0.183		
HB71	FAKKLAKKLKKLAKKLAK-COOH	18	2055.71	10.90	9	5.1	0.714		
P5	RIVQRIKKWLLKWKKLGY	18	2356.98	11.26	7	45.5	0.58		65
P6.2	GLLRKWGKKWKEFLRRVWK	19	2515.09	11.75	7	32.8	0.793		
ZY4	VCKRWKKWKRKWKKWCV-NH_2	17	2377.00	10.74	9	32.8	0.745		66
Esc (1−21)	GIFSKLAGKKIKNLLISGLKG-NH_2	21	2185.72	10.60	5	41.3	0.188	respiratory (bacterial solution)	67
Esc (1−21)-1c	GIFSKLAGKKIKNlLIsGLKG-NH_2	21	2185.72	10.60	5	41.3	0.188		
WLBU2-D8	RRWVRRvRRWvRRvvRvvRRWvRR	24	3398.0	13.08	13	14.1	0.789		68
LL-37	LLGDFFRKSKEKIGKEFKRIVQRIKDFLRNLVPRTES	37	4493.32	10.61	6	20.1	0.521		67
IK8L	IRIKIRI	7	911.20	12.01	n.d.	n.d.	n.d.		72
LN-7	LRRWLRWLLRWMR-NH_2	13	1941.42	12.60	5	74.8	0.875	dental caries	78
GH12	GLLWHLLHHLLH-NH_2	12	1488.80	7.10	0	108.1	0.399		80, 82
BAR	NH_2-LEAAPKKVQDLLKKANITVKGAFQLFS-COOH	27	2958.54	9.83	3	34.8	0.434	periodontitis	85, 89
Nal-P-113	Ac-AKR-Nal-Nal-GYKRKF-Nal-NH_2	12	n.d	n.d	n.d	n.d	n.d		92

[a]The physicochemical properties when not disclosed by the original article were calculated on the Heliquest server (http://heliquest.ipmc.cnrs.fr/). Molecular weight and isoelectric points were obtained through the ProtParam Expasy server (https://web.expasy.org/protparam/). Lower case letters represent D-amino acids. X_1: 4-*t*-butylphenylalanine. NAL: β-naphthylalanines. n.d.: not determined due to the presence of unnatural amino acid residues or chemical modifications or too short input sequences. [b]Amino acid residues. [c]Theoretical molecular weight. [d]Theoretical isoelectric point. [e]Hydrophobicity (%). [f]Hydrophobic moment.

https://dx.doi.org/10.1021/acsptsci.0c00191
ACS Pharmacol. Transl. Sci. 2021, 4, 55−73

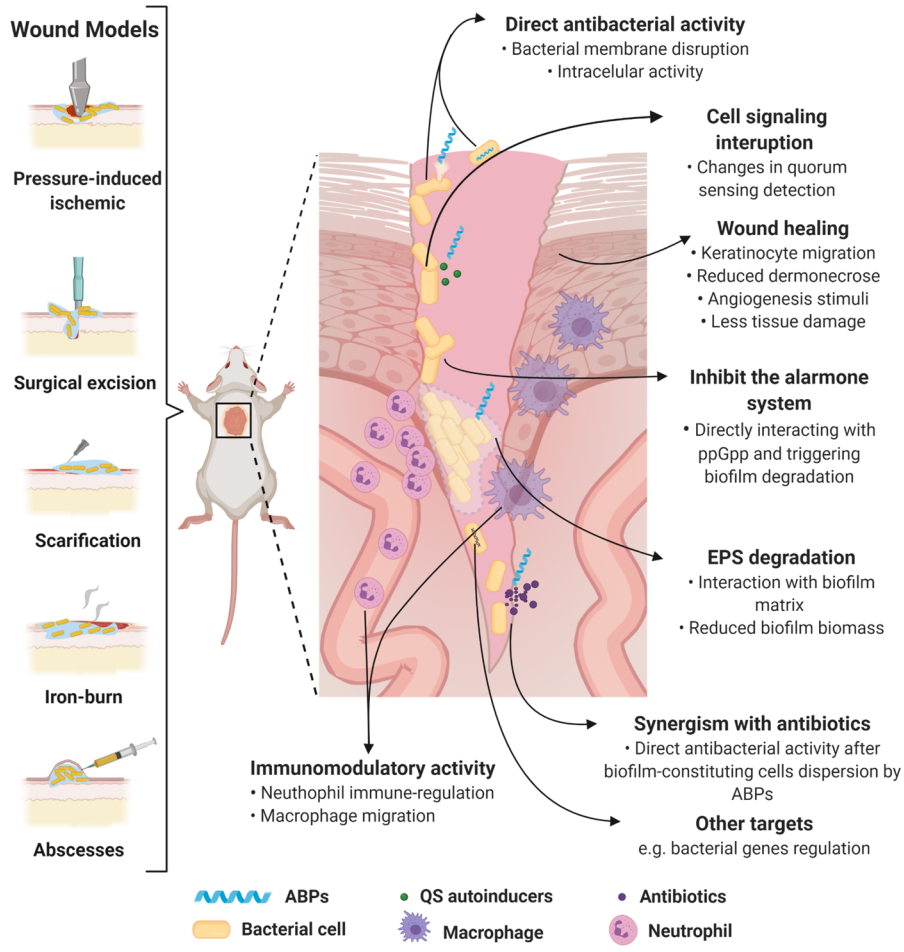

Figure 1. Murine biofilm wound models and proposed ABPs' modes of action. Biofilm wound models can be obtained by performing lesions on the animal's skin using different techniques (*e.g.*, surgical excision, skin scarification, iron-burn, and pressure), followed by the bacterium inoculum. Moreover, this model can be established by the bacterium's direct inoculum subcutaneously (*e.g.*, abscess). ABP treatment routes include topical and systemic administration. ABPs can assist in tissue recovery through mobilizing keratinocytes, stimulating angiogenesis, and reducing dermonecrosis. They can also display direct bactericidal effects alone or in synergism with antibiotics through membrane-associated mechanisms or acting intracellularly. ABPs also block cell signaling and communication, thus regulating biofilm-related gene transcription, impairing biofilm formation. In preformed biofilms, ABPs cause EPS degradation, detaching bacterial cells from surfaces and interfering with biofilm morphology. Finally, many ABPs act as immunomodulators, avoiding an exacerbated response mediated by cells (*e.g.*, neutrophil and macrophage), and assisting in recruiting cells (*e.g.*, keratinocytes) that assist wound healing. All figures were made by the authors with a subscription version of BioRender.com.

et al. (2017).[23] They used a preformed matrix in bacterial biofilms that were attached to the wound site and demonstrated biofilm proliferation. Moreover, in skin abscess models, the authors demonstrated genetic patterns as the presence of genes involved in EPS biosynthesis (*pslD*) and upregulation of EPS alginate synthesis (*mucC*) that are present in biofilm formation.[22] These models have assisted the identification of wound biofilm infection patterns (at the gene level) with greater representativeness and translational potential for preclinical tests.

The topical route is the most used and presents the most effective results when evaluating ABPs *in vivo*. The systemic route has also been used;[21,23,26,29,34] however, the results obtained were not as promising as those from topical administration studies, as ABPs usually present low bloodstream stability, rendering them inactive.[10] As described above and reported by Kłodzińska et al. (2019)[35] and Kumar et al. (2019),[36] nanoencapsulation strategies can improve the bioavailability of ABPs, favoring the translation of these antibiofilm agents into the clinic.

FOREIGN BODY INFECTION MODEL

Among the most commonly colonized medical devices are urinary catheters, cardiac pacemakers, dental implants, vascular prostheses, peritoneal dialysis catheters, stents, intrauterine devices, contact lenses, and breast implants.[38] The presence of a foreign body significantly increases biofilm formation, as this exogenous structure offers an ideal surface for bacterial growth. Additionally, the foreign body can impair defense cells' functions, including leukocytes, thus facilitating bacterial adhesion and growth.[39]

Animal models using foreign bodies can be divided into two broad groups, the (i) site-specific device models that are inserted into a given organ or are arranged in similar regions in humans (*e.g.*, urinary stents, venous catheters, prosthetic implants) and (ii) subcutaneous device models (*e.g.*, cage tissue, catheters subcutaneously) (Tables 1 and 2).[38] Moreover, it is common to find studies evaluating ABPs' stability in body fluids, including blood, urine, among others, prior to *in vivo* experiments. These *in vitro* assays allow a better understanding of ABPs' behavior in different biological conditions, contributing to a more robust

https://dx.doi.org/10.1021/acsptsci.0c00191
ACS Pharmacol. Transl. Sci. 2021, 4, 55−73

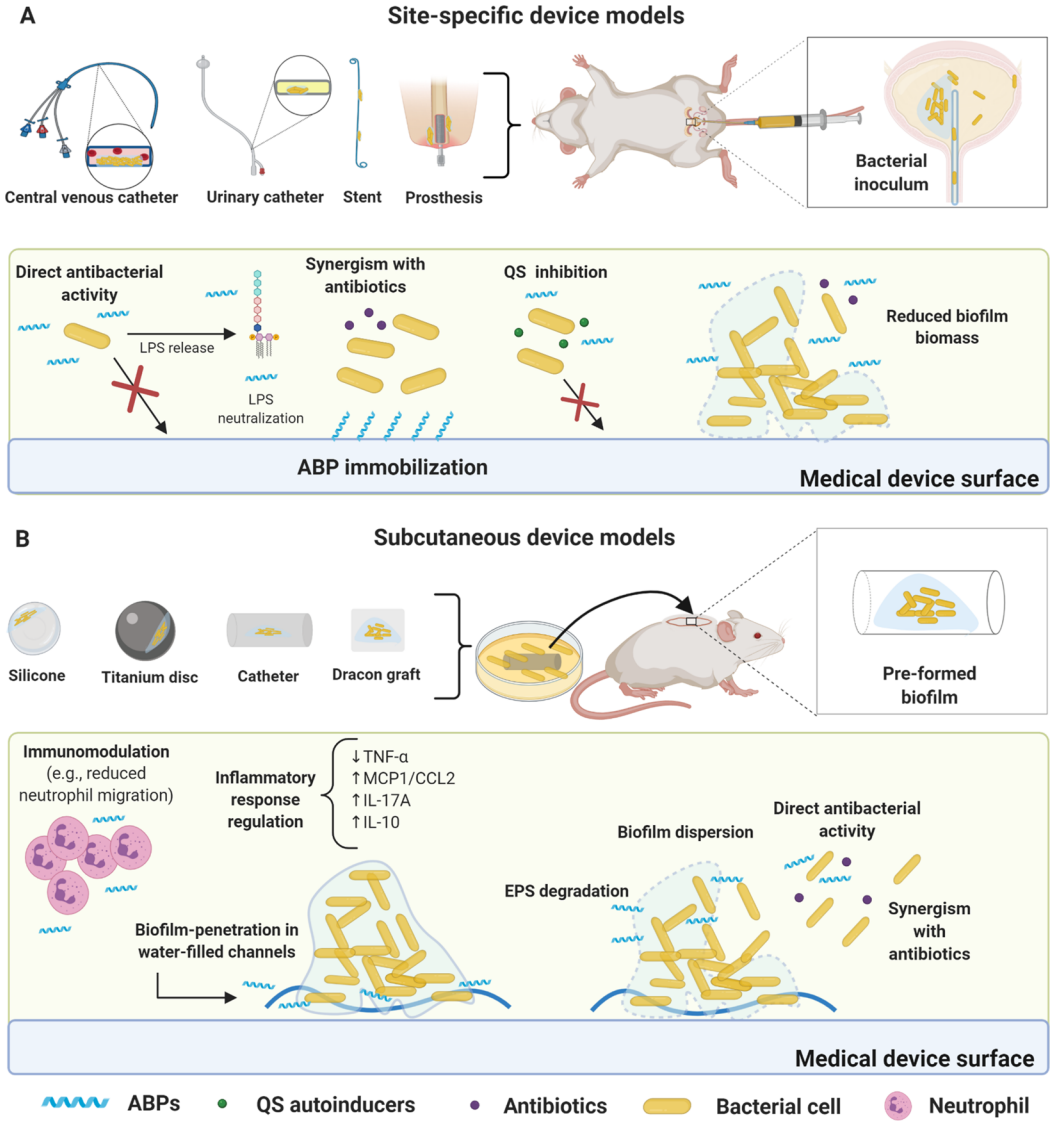

Figure 2. Foreign body murine models for biofilm infections and proposed ABPs modes of action. (A) Site-specific device model. The most common devices used to assess ABPs activity include catheter and urinary stents, central venous catheters (CVC), and periprosthetic implants, all surgically inserted. ABPs can be immobilized on the device's surface, thus inhibiting biofilm formation for extended periods. This strategy can be used in association with conventional antibiotics. Some ABPs also inhibit bacterial communication (*e.g.*, QS). Direct bacterial activity is also a common mechanism (*e.g.*, ABPs alone or in synergism with antibiotics) for inhibiting biofilm formation. In preformed biofilms, ABPs can reduce biofilm biomass. Furthermore, direct bacterial activity is also a common mechanism. (B) Subcutaneous device models. In these models, biofilm is usually previously formed in the device (*e.g.*, titanium disc, silicone beads, Dracon graft, and catheter). The infected device is inserted subcutaneously in the animal (mouse or rat), followed by ABP treatment. ABPs have demonstrated direct antibacterial activity in most cases with bacterial membrane disruption. The antibiofilm activity has also been achieved via EPS degradation, leading to biofilm dispersion and enabling synergism with antibiotics. Additionally, ABPs have been shown to penetrate the biofilms through water channels and disperse biofilm cells, followed by direct antibacterial effects. Immunomodulatory responses have also been observed, including reduced neutrophil migration and cytokine regulation (*e.g.*, TNF-α, MCP1/CCL2 IL-17A, and IL-10). All figures were made by the authors with a subscription version of BioRender.com.

assessment of the possible mechanisms involved in their antibiofilm activities *in vivo*.

Site-Specific Device Models. The abiotic nature of medical devices favors biofilm proliferation, as a considerably lower bacterial load is sufficient to colonize these devices, triggering chronic infections and even systemic infections.[40,41] In this model, the bacterial load is injected at the infection site after the device implantation surgery (*e.g.*, central venous catheters (CVC), urinary catheter, and stent).[42,43] ABPs have been used alone or in synergy with antibiotics before or after the infection is established (Tables 1 and 2). The antibiofilm potential of mono- and combination therapies is measured by bacterial recovery from the infection site or the portion of the device where bacteria were attached. Notably, in the case of the urinary stent case, bacteria can be detected in the urine, whereas in the CVC model, the peripheral blood can be collected and analyzed for quantifying bacterial load (Figure 2 A).[42,43]

Many *in vivo* models have been proposed to help approximate experimental conditions from those found in urinary tract infections. ABPs have been widely evaluated as alternatives to combat urinary tract infections. For instance, the activity of teicoplanin combined with RIP has been assessed against *S. aureus* biofilms by coating urinary stents with peptide and surgically implanting them in the bladder of rats.[43]

https://dx.doi.org/10.1021/acsptsci.0c00191
ACS Pharmacol. Transl. Sci. 2021, 4, 55−73

The use of CVC is also associated with biofilms, aggravating difficult-to-treat infections.[44] Antibiotics become ineffective against infected CVC because of biofilm attachment to the device wall.[40] Therefore, several studies have used *in vivo* CVC models to investigate prospective antibiofilm compounds.[45] For instance, to evaluate the activity of the peptide citropin1.1 (Table 2), Cirioni et al. (2016)[42] used a CVC that was inserted into the jugular vein of rats and advanced to the superior vena cava. A pretreatment was performed by filling the catheters with citropin1.1 alone or in combination with antibiotics, followed by infection with *S. aureus*. The authors demonstrate that citropin1.1 alone and combined with minocycline and rifampicin reduced the bacterial load. The authors suggest that citropin1.1 acts by inhibiting *S. aureus* adherent cell growth, allowing antibiotics to act on planktonic bacterial cells, thus inhibiting biofilm formation.[42]

Similarly, a CVC model in rats was used to evaluate the activity of the cathelicidin BMAP-28 (Table 2). Catheters pretreated with BMAP-28 in conjunction with antibiotics (quinupristin/dalfopristin (Q/D), linezolid, and vancomycin) displayed a 4-log reduction in bacterial load with no observation of bacteremia.[46] Moreover, Ghiselli et al. (2007)[47] demonstrated that, by combining the peptide protegrin IB-367 with linezolid, a significant decrease in *S. aureus* and *E. faecium* bacterial load (and no bacteremia) was observed.[47]

Treatment of periprosthetic joint infections is scarce and usually requires surgical interventions and long-term antibiotic therapy, presenting high mortality rates.[48] A periprosthetic joint infection mouse model was used to evaluate the activity of peptide WLBU2 (Table 2) in eliminating implant-associated biofilms.[49] The bacterial load reduction was dose-dependent at 0.01 and 10 mg kg^{-1}. Additionally, this peptide demonstrated low toxicity and high stability, making it a valuable candidate for antibiofilm treatment in prosthetic implants.[49]

Subcutaneous Device Models. Subcutaneous implant models are widely used in biofilm-related infections and to assess the efficacy of ABPs, since the surgical incision on the animal's back is more accessible than the implantation of local devices.[38] Various materials with different textures can be implanted (*e.g.*, titanium, silicone, Dacron graft, and catheter), directly influencing bacterial load recovery and local inflammatory responses.[40] In the foreign body subcutaneous device models, a surgical incision is made on the back of the animal, where the device is inserted subcutaneously (Figure 2 B). Most studies using ABPs in the context of subcutaneous device models evaluate their effects on preformed biofilms.[50−53] Consequently, in these studies, it is imperative to guarantee that the bacteria are at the mature biofilm stage prior to treatment.

ABPs can also be immobilized on the device's surface prior to the infection and surgery, with the overarching goal of preventing bacterial attachment and further biofilm formation. Recovered bacterial counts are typically utilized as a proxy for treatment effectiveness. However, histological analysis, imaging by IVIS, scanning microscopy, and inflammatory response detection are also used as critical parameters in these models (Table 1).[50−53]

Minardi et al. (2007)[50] reported that tachyplesin III-coated urethral stents were used to eradicate *P. aeruginosa* infections in rat subcutaneous pouch models, inhibiting biofilm growth up to 1000 times compared to untreated controls.[50] Similarly, Lee et al. (2019)[54] showed that peptide HPA3NT3 (Table 2) reduced biofilm formation, tissue damage, and toxicity (Table 1). Using the same model, Ma et al. (2020)[53] used a catheter infected with preformed *P. aeruginosa* biofilm, which was further inserted subcutaneously in mice to evaluate the antibiofilm activity of peptide EC1-17KV (Tables 1 and 2). This same model was used to demonstrate the antibiofilm potential of ABP 17tF-W (Tables 1 and 2), a peptide derived from LL-37, on MRSA biofilms. In addition to combating biofilms, this peptide exhibited immunomodulatory activity and resistance to proteases.[55] Chen et al. (2016)[51] described the activity of the ABP melamine (Table 2) as a titanium coating agent in a subcutaneous infection mouse model. The titanium surface was functionalized via a series of reactions that yielded a thioether linkage between the functionalized surface and the sulfhydryl group of melimine. The AMP-coated material significantly reduced biofilm formation by *P. aeruginosa* in both mouse and rat subcutaneous infection models and reduced the bacterial load by up to 2-log compared to the uncoated titanium surface (Table 1).

The model with Dacron grafts has also been used to evaluate ABPs. Soon after the Dacron grafts were pretreated with ABPs, including RIP, 13-residue dermaseptin derivative (DD13), and hybrid DD13-RIP, they were inserted in the subcutaneous pockets. All three peptides reduced the graft's bacterial load (from 3 to 4-log), with DD13-RIP demonstrating the best results (5-log reduction) at a lower dose (10 mg L^{-1}) (Tables 1 and 2). Moreover, these peptides demonstrated synergism with the antibiotic rifampicin, boosting its activity against resistant strains.[56]

Yu et al. (2020)[52] demonstrated that supramolecular coassembly with mesoporous silica nanoparticles improved delivery of antibiotics and the peptide melittin. This strategy led to enhanced antibiofilm activity *in vitro* and in a preformed biofilm model of *P. aeruginosa* in subcutaneous silicone implants. Additionally, it prevented tissue damage and inflammation associated with the implant.[52] Moreover, Ju et al. (2020)[57] proposed a chitosan-polyethylene (CS-PEG) glycol-peptide (LK13 peptide) conjugate (CS-PEG-LK13) targeting the biofilm water channels and the negative charge of EPS (Figure 2B). The authors demonstrate that these characteristics allowed the penetration of this conjugate into biofilms and, subsequently, increased antibacterial activity compared to the LK13 (Table 2) alone. These conjugates' effectiveness was also demonstrated in a murine model of subcutaneous implantation of silicone sheets infected with preformed *P. aeruginosa* biofilms.[57]

RESPIRATORY TRACT CHRONIC INFECTION MODELS

P. aeruginosa is considered the primary agent responsible for biofilm lung infection in cystic fibrosis.[58,59] The biofilm mode of growth hinders complete eradication of the infection, leading to chronic inflammation of the subject's airways.[59] Some ABPs have been described for their activity in respiratory tract infection murine models (Tables 1 and 2).

In the CF murine model, bacteria may be inoculated through instillation, intranasally, or intratracheally.[60−62] In these models, the infection severity is determined by the inoculum and inoculation frequency of bacteria. The establishment of chronic pulmonary infection models can be obtained by using bacteria carriers (*e.g.*, alginate) produced by the bacterial strain itself or by bacterial incorporation onto agar beads (Table 1). In these cases, intratracheal instillation is the most appropriate route for bacterial inoculation.[63,64]

Some studies also use *P. aeruginosa* clinical isolates from CF patients (*e.g.*, bacterial solution) to evaluate the efficacy of ABPs (Tables 1 and 2). In these models, the time between infection establishment and the end of the treatment is much shorter than when bacteria are incorporated into agar, alginate, or silicone.

https://dx.doi.org/10.1021/acsptsci.0c00191
ACS Pharmacol. Transl. Sci. 2021, 4, 55−73

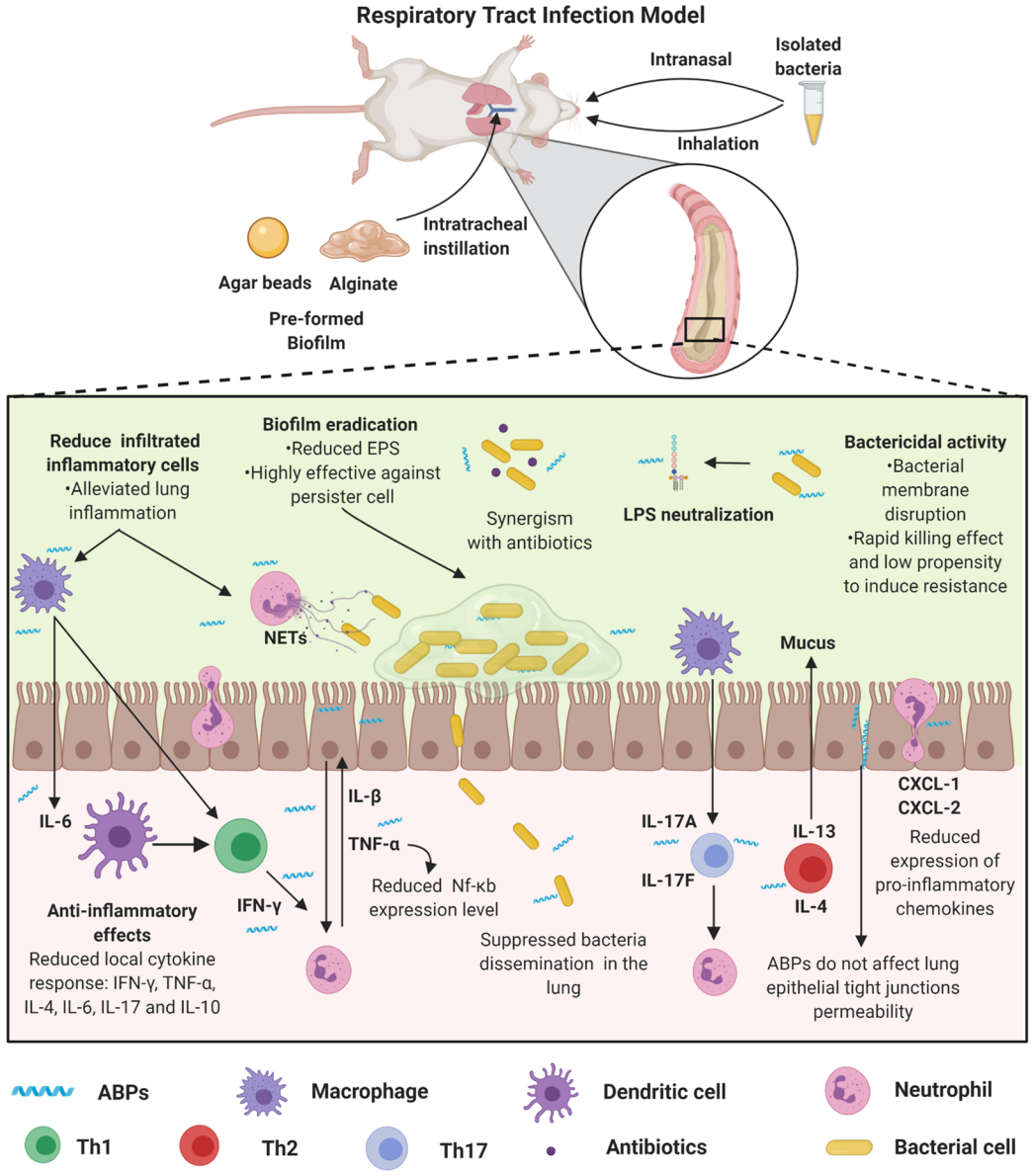

Figure 3. Respiratory tract biofilm infection models and proposed ABPs modes' of action. Respiratory tract biofilm infection models can be obtained by the incorporation of the bacteria in agar or alginate, which is instilled intratracheally, or a solution containing the biofilm-forming bacteria, which are inoculated directly into the animals' nostrils or by inhalation. These models simulate a process similar to cystic fibrosis. In this process, both the innate and adaptive immune systems promote an exacerbated response mediated by immune cells (*e.g.,* neutrophil, macrophage, dendritic cell, and lymphocytes), cytokines (*e.g.,* IFN-γ, TNF-α, IL-4, IL-6, IL-17, and IL-10), and chemokines (*e.g.,* CXCL-1 and CXCL-2). Therefore, ABPs have been used as immunomodulators. Some ABPs regulate the migration of inflammatory cells, including neutrophils, also acting by modulating the cytokine-mediated inflammatory response and reducing pro-inflammatory cytokines (*e.g.,* IL-6 and TNF-α, IL-1β). These activities may be associated with both increased survival after treatment with ABPs and reduced lung tissue damage in treated animals. Additionally, these peptides demonstrate potent antibacterial activity (alone or in synergism with antibiotics) and antibiofilm, along with LPS neutralization. All figures were made by the authors with a subscription version of BioRender.com.

This shorter treatment time is because the animals get worse since the bacteria is directly inoculated, which can progress to severe acute respiratory syndrome (SARS), leading to animal death even before the treatment has been effective (Figure 3).

Song et al. (2005)[63] reported a rat model in which the ABP novispirin G10 (Table 2) was administered intratracheally to treat *P. aeruginosa* mucoid biofilm lung infection. Compared to the control groups, the remaining bacteria in the lung between 3 and 5-days postinfection were reduced by 170 to 330 times in novispirin G10-treated mice (Table 1). Consistent with these results, in pulmonary pathological analysis, treated animals' lungs showed milder lesions and lower cytokine-mediated responses.[63]

Zhang et al. (2005)[60] performed a screening with 150 AMPs against clinical CF isolates, among which four peptides (HBCM2, HBCM3, HBCPα-2, and HB71) showed higher antibacterial and antibiofilm activity (Tables 1 and 2). These peptides were evaluated in a murine model of pulmonary biofilm infection with *P. aeruginosa*. The peptides HBCM2, HBCM3, HBCPα-2, and HB71 significantly reduced *P. aeruginosa* counts in the lung. Additionally, anti-inflammatory responses were also observed for HBCM2.[60] More recently, Martinez et al. (2020)[65] described two peptides, P5 and P6 (Table 2), with antibiofilm activity and effectiveness in treating pulmonary infection by *P. aeruginosa*. Moreover, these peptides also demonstrated anti-inflammatory

https://dx.doi.org/10.1021/acsptsci.0c00191
ACS Pharmacol. Transl. Sci. 2021, 4, 55−73

activity and led to reduced pro-inflammatory cytokines in the lung.[65]

The cyclic peptide ZY4 (Table 2) described by Mwangi et al. (2019)[66] demonstrated *in vitro* and *in vivo* effectiveness, high stability in plasma, and prolonged half-life. Additionally, this peptide inhibited MDR *P. aeruginosa* biofilm formation.[66] The pulmonary infection model with MDR *P. aeruginosa* was used to evaluate ZY4 *in vivo*. Bacteria were inoculated intranasally, and the treatment was carried out intravenously. The authors observed that ZY4 reduced 90% of the lungs' bacterial load at a concentration of 8 mg kg^{-1} (Table 1). Similarly, Chen et al. (2017)[67] reported the *in vivo* therapeutic efficacy of the Esc(1−21)-1c peptides (Table 2) against *P. aeruginosa*-induced pulmonary infection in a mouse model after a single, low-dose intratracheal instillation. The authors also showed that the peptides reduced the lung bacterial burden by 2-log, with a concomitant reduction in leukocyte recruitment and attenuated inflammatory response.

Here, we described the use of WLBU2 to treat biofilm-associated periprosthetic implant infections. WLBU2 has also been used to treat *P. aeruginosa* infections in a murine model of pulmonary infection. This peptide reduces pulmonary bacterial load and inflammation, with a single dose of 0.05 mg kg^{-1} instilled directly into the animals' lungs (Table 1). Additionally, this peptide is effective against bacteremia induced by *P. aeruginosa in vivo*. Recently, it was demonstrated the structural optimization of WLBU2 by D-amino acids insertion, thus improving this peptide's stability and reducing its toxicity *in vivo*.[68]

K. pneumoniae can also form a biofilm in tissues such as the lungs.[69] Additionally, this bacterium is widely found in respiratory devices (*e.g.*, mechanical ventilation system),[70] resulting in pulmonary infections in the lower respiratory tract. In a study by Guilhen et al. (2019),[71] a robust murine pneumonia model was established, revealing that free-floating bacteria dispersed from *K. pneumoniae* biofilms are associated with this bacterium colonization capacity, also compromising the host's immune system.[71]

In this context, a murine model of pneumonia was used to assess the ABP's activity, IK8L (Table 2).[72] In that study, the authors monitored the pulmonary infection evolution with bioluminescent bacteria instillation. Moreover, the antibiofilm effect of IK8L was accessed over time using a biphotonic imaging (Caliper's Xenogen IVIS XRII optical imaging technology) system. IK8L inhibited biofilm formation and modulated the inflammatory response mediated by inflammatory cytokines (*e.g.*, TNF-α, IL-6, and IL-1β) in the bronchoalveolar fluid (Table 1). Furthermore, IK8L interfered with signaling proteins (*e.g.*, STAT3, JAK2, and ERK1/2) that regulate IL-6, significantly reducing the animal's mortality.[72]

■ ORAL INFECTIONS MODELS

Dental caries is formed by diverse biofilms from pathogenic and commensal microorganisms. This disease is driven by diet and microbiota−matrix interactions that occur on the oral surface.[73] Moreover, ABPs have been explored as potent oral therapeutic agents.[74,75]

Dental caries is commonly reproduced in animal models using recently weaned rats (Figure 4A). To establish a dental infection, previous treatment with antibiotics is necessary to eliminate the existing microbiome. Subsequently, the animals are fed with cariogenic diets and, in parallel, they receive the bacteria orally (*e.g.*, *Streptococcus mutans*) in a period of 5−7 days, daily.[76,77] The infection can be confirmed by sowing oral samples. The topical treatment with the peptides is carried out on the teeth, daily, for 30−45 days. At the end of the experiment, the animals' mandibles and molars are excised to determine the carious lesions. Scanning electron microscopy analyses are also used in some studies (Table 1).[76−78]

Recently, the dental caries model described above was used to evaluate the LN-7 peptide (Table 2).[78] This peptide is derived from two bacteriocins, called reutericin 6 and/or gassericin A, which had known antibacterial and antibiofilm activities *in vitro*. In animal models, LN-7 was capable of significantly reducing dental injuries, at 32 μM, by efficiently suppressing the development of dental caries promoted by *S. mutans* biofilms.[78]

Similarly, the ABP GH12 (Table 2) has been reported for its potent antibacterial activity and antibiofilm activities, also reducing EPS and lactic acid *in vitro*.[79−81] This peptide (at 8 mg L^{-1}), when evaluated in a caries animal model infected with *S. mutans* not only reduced the incidence but also the severity of caries in rats (Table 1).[82] More recently, this same ABP was evaluated at a higher dose (64 mg L^{-1}), leading to the regulation of the dental plaque microbiota. It was observed that the abundance of commensal species was positively regulated, whereas cariogenic bacteria were negatively regulated. In addition, more accurate analyses, including the assessment of sulcal caries and dental surface, revealed that such damages were controlled by GH12 under cariogenic conditions.[83]

Other types of oral pathologies can be associated with biofilm formation. For example, periodontitis is triggered by an oral inflammatory dysfunction caused, mainly, by microbial biofilms formation in the subgingival region.[84,85] Biofilm formation in periodontitis is driven by interactions between different bacteria, including *Porphyromonas gingivalis* and oral streptococci species (*e.g.*, *Streptococcus oralis* and *Streptococcus gordonii*).[84,86,87] Therefore, *in vivo* models have been established to mimic periodontitis in mice (Figure 4 B). Infections with periodontitis-related bacteria (*e.g.*, *S. gordonii*, *P. gingivalis*) are performed orally and can be confirmed by oral sowing or PCR analysis. The treatment can be carried out topically either for prevention or to eliminate an established biofilm infection. At the end of the experiment, the animals are euthanized and the skull is excised for alveolar bone loss analysis of the maxilla.[85,88,89]

Some ABPs have been tested in the above-mentioned periodontitis model (Tables 1 and 2). Numerous studies have shown that *P. gingivalis* biofilm formation requires an interaction with oral streptococci. Based on this, Daep et al. (2006)[84] developed a synthetic peptide, denominated BAR (Table 2), capable of inhibiting *P. gingivalis* and *S. gordonii* interaction, thus preventing biofilm formation *in vitro*.[84] Years later (2011),[85] those authors used a periodontitis mouse model in which both *S. gordonii* and *P. gingivalis* were used to simulate oral human periodontitis.[85] As a result, the BAR peptide showed promising *in vivo* activity by significantly preventing alveolar bone loss (Table 1), which is known to be the main consequence in periodontitis.[85]

More recently, that same peptide (BAR) was immobilized on poly(lactic-*co*-glycolic acid) nanoparticles surface, configuring nanoparticle−peptide complex BAR-modified NPs (BNPs).[89] This nanoformulation led to *in vivo* antibiofilm potential in a *S. gordonii* and *P. gingivalis* infection mouse model at lower doses (0.7 μM) than nonformulated BAR (3.4 μM).[89] In addition, BNPs have been shown to significantly reduce bone loss and IL-17 expression (Table 1),[89] an important gingival inflammatory mediator in *P. gingivalis* associated infections. Therefore, BNPs have proved to be strong candidates for the prevention and

https://dx.doi.org/10.1021/acsptsci.0c00191
ACS Pharmacol. Transl. Sci. 2021, 4, 55−73

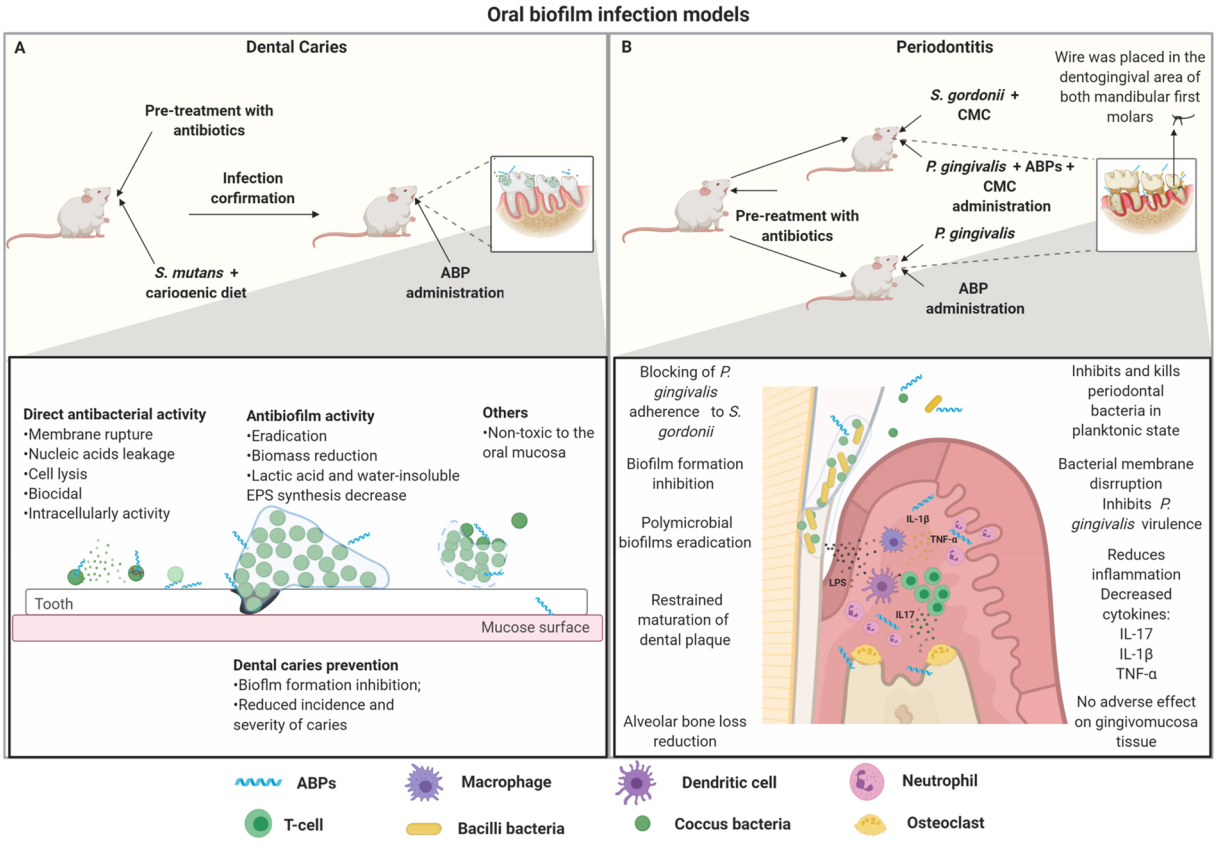

Figure 4. Oral biofilm infection model and proposed ABPs modes of action. (A) Dental caries infection model. In this model, some important factors are considered, including the use of newly weaned animals, pretreatment with antibiotics, confirmation of oral microbial depletion, and cariogenic diets in association with oral *S. mutans* infection. After the infection is confirmed, the topical treatment with ABPs is initiated. ABPs used in this model have been capable of preventing and eradicating biofilm-associated caries. ABPs can prevent tooth caries by inhibiting bacteria adherence to the tooth surface. In addition, ABPs also present direct antibacterial activity, significantly killing cariogenic pathogens before biofilm formation. When it comes to preformed biofilms, ABPs can interfere with the biofilm's structure by avoiding EPS synthesis and reducing biofilm biomass. (B) Periodontitis murine model. Periodontitis mainly consists of inflammation of the periodontium due to biofilm formation. Particularly, *S. gordonni* and *P. gingivalis* have been shown to play a crucial role in this infection. Usually, the primary colonization of *S. gordonni* is followed by the infection with *P. gingivalis*, using carboxymethylcellulose (CMC) as a vehicle. *P. gingivalis* can also be used alone to induce oral infection. However, in this case, there is a subgingival thread in the first molars from the mice to allow biofilm formation. ABPs have demonstrated the ability to prevent biofilm formation by acting directly on free-floating bacteria or eradicating preformed biofilms. ABPs can also modulate cytokines regulation (*e.g.*, IL-17, IL-1β, TNF-α), which significantly contributes to reducing alveolar bone loss, one of the main aggravating factors associated with periodontitis. All figures were made by the authors with a subscription version of BioRender.com.

prophylaxis of *P. gingivalis* biofilms in periodontitis. This nanoformulation strategy could be applied, for example, for mouthwashes or gels development.[89]

Another ABP, named Nal-P-113 (Table 2), has also demonstrated preventive periodontitis activity in rats' lower molars. Previous studies have already demonstrated that Nal-P-113 is stable in saliva and presents antibacterial and antibiofilm activity.[90,91] When evaluated in a periodontitis rat model, this peptide showed preserved biological potential toward pathogenic bacteria, also demonstrating anti-inflammatory activity by modulating cytokines production (IL-1β and TNF-α) and reducing alveolar bone loss (Table 1).[92] Interestingly, in that study,[92] biofilm formation was demonstrated using a 0.2 mm wire inserted in the dentogingival region of the lower first molars from rats. At the end of the experiment, this wire was removed and evaluated for biofilm formation through scanning electron microscopy. This strategy allowed the evaluation of the direct *in vivo* antibiofilm properties of Nal-P-113 against *P. gingivalis* associated with cocci bacteria and *Bacillus brevis*. Additionally, this technique allowed adherent bacteria recovery in their biofilm state and, through absolute quantitative real-time PCR analyses, it was possible to quantify the bacteria.[92] The peptide Nal-P-113 has already been submitted to clinical studies for the treatment of patients with chronic periodontitis, showing promising results in the inhibition of periodontal pathogens (*e.g.*, *P. gingivalis*, *Treponema denticola*, *Fusobacterium nucleatum*, and *S. gordonii*), also effectively countering oral biofilms.[93]

CHALLENGES IN TRANSLATING ABPS TO THE CLINIC

Preclinical studies are enabled by the development of robust animal models that are clinically significant.[94] When it comes to biofilm infections, it is often difficult to demonstrate biofilm formation and maintenance accurately and convincingly. However, as biofilms are notoriously present in chronic infections, different animal models have been used to evaluate antibiofilm compounds in preclinical trials, as described above.[95]

Most studies with ABPs include basic research and/or proof-of-concept studies. Consequently, there is a discrepancy between the volume of published studies and preclinical and clinical trials using ABPs. Currently (October 2020), according to the Biofilm-active

https://dx.doi.org/10.1021/acsptsci.0c00191
ACS Pharmacol. Transl. Sci. 2021, 4, 55−73

AMPs Database (BaAMPs), a total of 221 ABPs have shown antibiofilm potential toward 116 different target microorganisms. However, none of these ABPs have yet reached advanced clinical trials. The delay in translating antibiofilm drug candidates into the clinic was recently reviewed by Rumbaugh et al. (2020),[95] revealing that most clinical studies for treating biofilms involve the repurposing of drugs or combination of FDA-approved drugs.

By searching for antibiofilm preclinical and clinical trials in ClinicalTrails.gov (filters: bacterial infections; biofilm), only 14 studies were found, none of which involved ABPs. One of the main limitations when translating ABPs to the clinic is the use of appropriate *in vivo* models for preclinical screening. Studies using ABPs present significant differences among them, most of which are due to the lack of experimental standardization.[96] Such differences include the bacterial load used, which can widely change the outcome of the study, since the use of a low bacterial load may lead to false-positive results in the treated animal group.

Some alternatives have been explored to overcome these obstacles. Many studies have adopted colorimetric reagents to monitor and demonstrate biofilm development, including using bioluminescent bacterial strains.[97] Moreover, a new biofilm infection model of shoulder implants has been reported, in which a noninvasive tracking of the biofilm was performed through optical images.[98] Additionally, specific biofilm features can be investigated to confirm their proper establishment, including *Gac* regulatory pathways, EPS production, and QS signaling.[62]

Although previous studies have already demonstrated the role of extracellular DNA (eDNA) in biofilm formation and increased resistance to antibiotics,[99,100] its role and location *in vivo* have not yet been fully clarified.[100,101] Recently, transmission electron microscopy in conjunction with laser confocal scanning was used to evaluate the interactions between *P. aeruginosa* biofilms and polymorphonucleated (PMNs) cells, also shedding light on the role and location of eDNA in a murine implant model.[102] Furthermore, a new model of murine keratitis biofilm was recently established and features such as the extracellular matrix were identified through fluorescence electron microscopy and transmission from the animals' cornea.[103]

In biofilms associated with chronic infections, a recent work has reported more robust models to achieve chronicity in animals.[38] Bayes et al. (2016)[64] developed a murine model of pulmonary biofilm infection adapted from agar beads using a clinical mucoid strain of *P. aeruginosa*. The authors demonstrated the transition from transient infection of airways to chronic infection. The animals were kept for 2 weeks to reproduce some of the characteristics observed in humans, including variable bacterial clearance, endobronchial infection, development of antipseudomonal antibodies, and low mortality in the acute infection phase.

In addition to these innovative *in vivo* models, well-established *in situ* screening can lead to more efficient products *in vivo* by reducing the unnecessary use of animals.[104] Techniques with 3D skin, cell culture from different tissues, and *ex vivo* models can be relevant alternatives for determining the activity of ABPs against biofilms.[9] Taken together, all these techniques contribute to the establishment of the 3Rs (Replacement, Reduction, and Refinement) aiming at the welfare of animals with less invasive techniques and the refinement of techniques to obtain clinically significant results for novel drug candidates specifically developed for biofilm infections.

CONCLUSIONS AND PROSPECTS

The multifactorial nature of biofilm infections and multidrug resistance poses a significant challenge when developing novel effective drugs. Therefore, the combination of multifactorial therapies with improved efficiency is needed. The selection of robust murine models that accurately mimic biofilm infections directly and significantly improves any study associated with ABPs. Indeed, many of these studies fail at the stage of selecting an appropriate animal model, thus compromising subsequent preclinical work. Moreover, even if the *in vivo* model adopted is adequate and the experiment is well designed, most studies to date have lacked pharmacokinetics and pharmacodynamics data. Another limiting factor for translating ABPs to the clinic is their high cost of synthesis. For preclinical and clinical trials, large amounts of raw peptide material are needed and, depending on the candidate and its therapeutic dose, these tests may not be viable. In summary, although some limitations still need to be overcome, here we describe the most appropriate and significant murine models for antibiofilm evaluation of peptide-based drug candidates and highlight recent advances that have contributed significantly to the evaluation of the lead ABPs described to date.

AUTHOR INFORMATION

Corresponding Authors

Octávio L. Franco − *S-Inova Biotech, Programa de Pós-Graduação Stricto Sensu em Biotecnologia, Universidade Católica Dom Bosco, Campo Grande, Mato Grosso do Sul 79117-010, Brazil; Centro de Análises Proteômicas e Bioquímicas, Pós-Graduação em Ciências Genômicas e Biotecnologia, Universidade Católica de Brasília, Brasília, Distrito Federal 71966-700, Brazil;* orcid.org/0000-0001-9546-0525; Email: ocfranco@gmail.com

Marlon H. Cardoso − *S-Inova Biotech, Programa de Pós-Graduação Stricto Sensu em Biotecnologia, Universidade Católica Dom Bosco, Campo Grande, Mato Grosso do Sul 79117-010, Brazil; Centro de Análises Proteômicas e Bioquímicas, Pós-Graduação em Ciências Genômicas e Biotecnologia, Universidade Católica de Brasília, Brasília, Distrito Federal 71966-700, Brazil;* orcid.org/0000-0001-6676-5362; Email: marlonhenrique6@gmail.com

Authors

Gislaine G. O. S. Silveira − *S-Inova Biotech, Programa de Pós-Graduação Stricto Sensu em Biotecnologia, Universidade Católica Dom Bosco, Campo Grande, Mato Grosso do Sul 79117-010, Brazil*

Marcelo D. T. Torres − *Machine Biology Group, Departments of Psychiatry and Microbiology, Institute for Biomedical Informatics, Institute for Translational Medicine and Therapeutics, Perelman School of Medicine, Departments of Bioengineering and Chemical and Biomolecular Engineering, School of Engineering and Applied Science, and Penn Institute for Computational Science, University of Pennsylvania, Philadelphia, Pennsylvania 19104, United States*

Camila F. A. Ribeiro − *S-Inova Biotech, Programa de Pós-Graduação Stricto Sensu em Biotecnologia, Universidade Católica Dom Bosco, Campo Grande, Mato Grosso do Sul 79117-010, Brazil*

Beatriz T. Meneguetti − *S-Inova Biotech, Programa de Pós-Graduação Stricto Sensu em Biotecnologia, Universidade Católica Dom Bosco, Campo Grande, Mato Grosso do Sul 79117-010, Brazil*

Cristiano M. E. Carvalho − *S-Inova Biotech, Programa de Pós-Graduação Stricto Sensu em Biotecnologia, Universidade*

https://dx.doi.org/10.1021/acsptsci.0c00191
ACS Pharmacol. Transl. Sci. 2021, 4, 55−73

Católica Dom Bosco, Campo Grande, Mato Grosso do Sul 79117-010, Brazil

Cesar de la Fuente-Nunez − *Machine Biology Group, Departments of Psychiatry and Microbiology, Institute for Biomedical Informatics, Institute for Translational Medicine and Therapeutics, Perelman School of Medicine, Departments of Bioengineering and Chemical and Biomolecular Engineering, School of Engineering and Applied Science, and Penn Institute for Computational Science, University of Pennsylvania, Philadelphia, Pennsylvania 19104, United States;* orcid.org/0000-0002-2005-5629

Complete contact information is available at: https://pubs.acs.org/10.1021/acsptsci.0c00191

Notes

The authors declare no competing financial interest.

■ ACKNOWLEDGMENTS

This work was supported by grants from Fundação de Apoio à Pesquisa do Distrito Federal (FAPDF), Coordenação de Aperfeiçoamento de Pessoal de Nível Superior (CAPES), Conselho Nacional de Desenvolvimento e Tecnológico (CNPq), and Fundação de Apoio ao Desenvolvimento do Ensino, Ciência e Tecnologia do Estado de Mato Grosso do Sul (FUNDECT), Brazil. C.d.l.F-N. holds a Presidential Professorship at the University of Pennsylvania, is a recipient of the Langer Prize by the AIChE Foundation, and acknowledges funding from the Institute for Diabetes, Obesity, and Metabolism, the Penn Mental Health AIDS Research Center of the University of Pennsylvania, and the National Institute of General Medical Sciences of the National Institutes of Health under award number R35GM138201.

■ REFERENCES

(1) Vert, M., Doi, Y., Hellwich, K.-H., Hess, M., Hodge, P., Kubisa, P., Rinaudo, M., and Schué, F. (2012) Terminology for Biorelated Polymers and Applications (IUPAC Recommendations 2012). *Pure Appl. Chem. 84*, 377−410.

(2) de la Fuente-Núñez, C., Reffuveille, F., Fernández, L., and Hancock, R. E. W. (2013) Bacterial Biofilm Development as a Multicellular Adaptation: Antibiotic Resistance and New Therapeutic Strategies. *Curr. Opin. Microbiol. 16*, 580−589.

(3) Dieltjens, L., Appermans, K., Lissens, M., Lories, B., Kim, W., Van der Eycken, E. V., Foster, K. R., and Steenackers, H. P. (2020) Inhibiting Bacterial Cooperation Is an Evolutionarily Robust Anti-Biofilm Strategy. *Nat. Commun. 11*, 107.

(4) Ahmed, M. N., Abdelsamad, A., Wassermann, T., Porse, A., Becker, J., Sommer, M. O. A., Høiby, N., and Ciofu, O. (2020) The Evolutionary Trajectories of *P. aeruginosa* in Biofilm and Planktonic Growth Modes Exposed to Ciprofloxacin: Beyond Selection of Antibiotic Resistance. *npj Biofilms Microbi. 6*, 28.

(5) Schrader, S. M., Vaubourgeix, J., and Nathan, C. (2020) Biology of Antimicrobial Resistance and Approaches to Combat It. *Sci. Transl. Med. 12*, eaaz6992.

(6) Koo, H., Allan, R. N., Howlin, R. P., Hall-Stoodley, L., and Stoodley, P. (2017) Targeting Microbial Biofilms: Current and Prospective Therapeutic Strategies. *Nat. Rev. Microbiol. 15*, 740−755.

(7) Verderosa, A. D., Totsika, M., and Fairfull-Smith, K. E. (2019) Bacterial Biofilm Eradication Agents: A Current Review. *Front. Chem. 7*, 824.

(8) Hughes, G., and Webber, M. A. (2017) Novel Approaches to the Treatment of Bacterial Biofilm Infections. *Br. J. Pharmacol. 174*, 2237−2246.

(9) de Breij, A., Riool, M., Cordfunke, R. A., Malanovic, N., de Boer, L., Koning, R. I., Ravensbergen, E., Franken, M., van der Heijde, T., Boekema, B. K., Kwakman, P. H. S., Kamp, N., El Ghalbzouri, A., Lohner, K., Zaat, S. A. J., Drijfhout, J. W., and Nibbering, P. H. (2018) The Antimicrobial Peptide SAAP-148 Combats Drug-Resistant Bacteria and Biofilms. *Sci. Transl. Med. 10*, eaan4044.

(10) Dostert, M., Belanger, C. R., and Hancock, R. E. W. (2019) Design and Assessment of Anti-Biofilm Peptides: Steps Toward Clinical Application. *J. Innate Immun. 11*, 193−204.

(11) Starr, C. G., Ghimire, J., Guha, S., Hoffmann, J. P., Wang, Y., Sun, L., Landreneau, B. N., Kolansky, Z. D., Kilanowski-Doroh, I. M., Sammarco, M. C., Morici, L. A., and Wimley, W. C. (2020) Synthetic Molecular Evolution of Host Cell-Compatible, Antimicrobial Peptides Effective against Drug-Resistant, Biofilm-Forming Bacteria. *Proc. Natl. Acad. Sci. U. S. A. 117*, 8437−8448.

(12) Pletzer, D., and Hancock, R. E. W. (2016) Antibiofilm Peptides: Potential as Broad-Spectrum Agents. *J. Bacteriol. 198*, 2572−2578.

(13) Di Somma, A., Moretta, A., Canè, C., Cirillo, A., and Duilio, A. (2020) Antimicrobial and Antibiofilm Peptides. *Biomolecules 10*, 652.

(14) Yasir, M., Willcox, M. D. P., and Dutta, D. (2018) Action of Antimicrobial Peptides against Bacterial Biofilms. *Materials 11*, 2468.

(15) Okuda, K., Zendo, T., Sugimoto, S., Iwase, T., Tajima, A., Yamada, S., Sonomoto, K., and Mizunoe, Y. (2013) Effects of Bacteriocins on Methicillin-Resistant *Staphylococcus aureus* Biofilm. *Antimicrob. Agents Chemother. 57*, 5572−5579.

(16) de la Fuente-Núñez, C., Korolik, V., Bains, M., Nguyen, U., Breidenstein, E. B. M., Horsman, S., Lewenza, S., Burrows, L., and Hancock, R. E. W. (2012) Inhibition of Bacterial Biofilm Formation and Swarming Motility by a Small Synthetic Cationic Peptide. *Antimicrob. Agents Chemother. 56*, 2696−2704.

(17) Libardo, M. D. J., Bahar, A. A., Ma, B., Fu, R., McCormick, L. E., Zhao, J., McCallum, S. A., Nussinov, R., Ren, D., Angeles-Boza, A. M., and Cotten, M. L. (2017) Nuclease Activity Gives an Edge to Host-Defense Peptide Piscidin 3 over Piscidin 1, Rendering It More Effective against Persisters and Biofilms. *FEBS J. 284*, 3662−3683.

(18) de la Fuente-Núñez, C., Reffuveille, F., Haney, E. F., Straus, S. K., and Hancock, R. E. W. (2014) Broad-Spectrum Anti-Biofilm Peptide That Targets a Cellular Stress Response. *PLoS Pathog. 10*, e1004152.

(19) Coenye, T., and Nelis, H. J. (2010) *In vitro* and *In vivo* Model Systems to Study Microbial Biofilm Formation. *J. Microbiol. Methods 83*, 89−105.

(20) Wu, Y.-K., Cheng, N.-C., and Cheng, C. M. (2019) Biofilms in Chronic Wounds: Pathogenesis and Diagnosis. *Trends Biotechnol. 37*, 505−517.

(21) Nakagami, G., Sanada, H., Sugama, J., Morohoshi, T., Ikeda, T., and Ohta, Y. (2008) Detection of *Pseudomonas aeruginosa* Quorum Sensing Signals in an Infected Ischemic Wound: An Experimental Study in Rats. *Wound Repair Regen. 16*, 30−36.

(22) Pletzer, D., Mansour, S. C., Wuerth, K., Rahanjam, N., and Hancock, R. E. W. (2017) New Mouse Model for Chronic Infections by Gram-Negative Bacteria Enabling the Study of Anti-Infective Efficacy and Host-Microbe Interactions. *mBio 8*, e00140.

(23) Chung, E. M. C., Dean, S. N., Propst, C. N., Bishop, B. M., and van Hoek, M. L. (2017) Komodo Dragon-Inspired Synthetic Peptide DRGN-1 Promotes Wound-Healing of a Mixed-Biofilm Infected Wound. *npj Biofilms Microbiomes 3*, 9.

(24) Thomsen, T. R., Aasholm, M. S., Rudkjøbing, V. B., Saunders, A. M., Bjarnsholt, T., Givskov, M., Kirketerp-Møller, K., and Nielsen, P. H. (2010) The Bacteriology of Chronic Venous Leg Ulcer Examined by Culture-Independent Molecular Methods. *Wound Repair Regen. 18*, 38−49.

(25) Roberts, A. E. L., Kragh, K. N., Bjarnsholt, T., and Diggle, S. P. (2015) The Limitations of *in vitro* Experimentation in Understanding Biofilms and Chronic Infection. *J. Mol. Biol. 427*, 3646−3661.

(26) Ma, Z., Han, J., Chang, B., Gao, L., Lu, Z., Lu, F., Zhao, H., Zhang, C., and Bie, X. (2017) Membrane-Active Amphipathic Peptide WRL3 with *in vitro* Antibiofilm Capability and *in vivo* Efficacy in Treating Methicillin-Resistant *Staphylococcus aureus* Burn Wound Infections. *ACS Infect. Dis. 3*, 820−832.

(27) Woodburn, K. W., Jaynes, J. M., and Clemens, L. E. (2019) Evaluation of the Antimicrobial Peptide, RP557, for the Broad-

Spectrum Treatment of Wound Pathogens and Biofilm. *Front. Microbiol. 10*, 1688.
(28) Torres, M. D. T., Pedron, C. N., Higashikuni, Y., Kramer, R. M., Cardoso, M. H., Oshiro, K. G. N., Franco, O. L., Junior, P. I. S., Silva, F. D., Junior, V. X. O., Lu, T. K., and Fuente-Nunez, C. de la. (2018) Structure-Function-Guided Exploration of the Antimicrobial Peptide Polybia-CP Identifies Activity Determinants and Generates Synthetic Therapeutic Candidates. *Commun. Biol. 1*, 221.
(29) Oshiro, K. G. N., Cândido, E. S., Chan, L. Y., Torres, M. D. T., Monges, B. E. D., Rodrigues, S. G., Porto, W. F., Ribeiro, S. M., Henriques, S. T., Lu, T. K., de la Fuente-Nunez, C., Craik, D. J., Franco, O. L., and Cardoso, M. H. (2019) Computer-Aided Design of Mastoparan-like Peptides Enables the Generation of Nontoxic Variants with Extended Antibacterial Properties. *J. Med. Chem. 62*, 8140−8151.
(30) Pane, K., Cafaro, V., Avitabile, A., Torres, M. D. T., Vollaro, A., De Gregorio, E., Catania, M. R., Di Maro, A., Bosso, A., Gallo, G., Zanfardino, A., Varcamonti, M., Pizzo, E., Di Donato, A., Lu, T. K., de la Fuente-Nunez, C., and Notomista, E. (2018) Identification of Novel Cryptic Multifunctional Antimicrobial Peptides from the Human Stomach Enabled by a Computational−Experimental Platform. *ACS Synth. Biol. 7*, 2105−2115.
(31) Cardoso, M. H., Cândido, E. S., Chan, L. Y., Der Torossian Torres, M., Oshiro, K. G. N., Rezende, S. B., Porto, W. F., Lu, T. K., de la Fuente-Nunez, C., Craik, D. J., and Franco, O. L. A (2018) Computationally Designed Peptide Derived from *Escherichia coli* as a Potential Drug Template for Antibacterial and Antibiofilm Therapies. *ACS Infect. Dis. 4*, 1727−1736.
(32) Cândido, E. S., Cardoso, M. H., Chan, L. Y., Torres, M. D. T., Oshiro, K. G. N., Porto, W. F., Ribeiro, S. M., Haney, E. F., Hancock, R. E. W., Lu, T. K., de la Fuente-Nunez, C., Craik, D. J., and Franco, O. L. (2019) Short Cationic Peptide Derived from Archaea with Dual Antibacterial Properties and Anti-Infective Potential. *ACS Infect. Dis. 5*, 1081−1086.
(33) Schierle, C. F., De la Garza, M., Mustoe, T. A., and Galiano, R. D. (2009) Staphylococcal Biofilms Impair Wound Healing by Delaying Reepithelialization in a Murine Cutaneous Wound Model. *Wound Repair Regen. 17*, 354−359.
(34) Mansour, S. C., Pletzer, D., de la Fuente-Núñez, C., Kim, P., Cheung, G. Y. C., Joo, H.-S., Otto, M., and Hancock, R. E. W. (2016) Bacterial Abscess Formation Is Controlled by the Stringent Stress Response and Can Be Targeted Therapeutically. *EBioMedicine 12*, 219−226.
(35) Kłodzińska, S. N., Pletzer, D., Rahanjam, N., Rades, T., Hancock, R. E. W., and Nielsen, H. M. (2019) Hyaluronic Acid-Based Nanogels Improve *in vivo* Compatibility of the Anti-Biofilm Peptide DJK-5. *Nanomedicine 20*, 102022.
(36) Kumar, P., Pletzer, D., Haney, E. F., Rahanjam, N., Cheng, J. T. J., Yue, M., Aljehani, W., Hancock, R. E. W., Kizhakkedathu, J. N., and Straus, S. K. (2019) Aurein-Derived Antimicrobial Peptides Formulated with Pegylated Phospholipid Micelles to Target Methicillin-Resistant *Staphylococcus aureus* Skin Infections. *ACS Infect. Dis. 5*, 443−453.
(37) Pletzer, D., Mansour, S. C., and Hancock, R. E. W. (2018) Synergy between Conventional Antibiotics and Anti-Biofilm Peptides in a Murine, Sub-Cutaneous Abscess Model Caused by Recalcitrant ESKAPE Pathogens. *PLoS Pathog. 14*, e1007084.
(38) Lebeaux, D., Chauhan, A., Rendueles, O., and Beloin, C. (2013) From *in vitro* to *in vivo* Models of Bacterial Biofilm-Related Infections. *Pathogens 2*, 288−356.
(39) Wu, H., Moser, C., Wang, H. Z., Høiby, N., and Song, Z. J. (2015) Strategies for Combating Bacterial Biofilm Infections. *Int. J. Oral Sci. 7*, 1−7.
(40) Khatoon, Z., McTiernan, C. D., Suuronen, E. J., Mah, T. F., and Alarcon, E. I. (2018) Bacterial Biofilm Formation on Implantable Devices and Approaches to Its Treatment and Prevention. *Heliyon 4*, e01067.
(41) Stewart, P. S., and Bjarnsholt, T. (2020) Risk Factors for Chronic Biofilm-Related Infection Associated with Implanted Medical Devices. *Clin. Microbiol. Infect. 26*, 1034−1038.
(42) Cirioni, O., Giacometti, A., Ghiselli, R., Kamysz, W., Orlando, F., Mocchegiani, F., Silvestri, C., Licci, A., Chiodi, L., Lukasiak, J., Saba, V., and Scalise, G. (2006) Citropin 1.1-Treated Central Venous Catheters Improve the Efficacy of Hydrophobic Antibiotics in the Treatment of Experimental Staphylococcal Catheter-Related Infection. *Peptides 27*, 1210−1216.
(43) Cirioni, O., Ghiselli, R., Minardi, D., Orlando, F., Mocchegiani, F., Silvestri, C., Muzzonigro, G., Saba, V., Scalise, G., Balaban, N., and Giacometti, A. (2007) RNAIII-Inhibiting Peptide Affects Biofilm Formation in a Rat Model of Staphylococcal Ureteral Stent Infection. *Antimicrob. Agents Chemother. 51*, 4518−4520.
(44) Gominet, M., Compain, F., Beloin, C., and Lebeaux, D. (2017) Central Venous Catheters and Biofilms: Where Do We Stand in 2017? *APMIS 125*, 365−375.
(45) Danese, P. N. (2002) Antibiofilm Approaches: Prevention of Catheter Colonization. *Chem. Biol. 9*, 873−880.
(46) Cirioni, O., Giacometti, A., Ghiselli, R., Bergnach, C., Orlando, F., Mocchegiani, F., Silvestri, C., Licci, A., Skerlavaj, B., Zanetti, M., Saba, V., and Scalise, G. (2006) Pre-Treatment of Central Venous Catheters with the Cathelicidin BMAP-28 Enhances the Efficacy of Antistaphylococcal Agents in the Treatment of Experimental Catheter-Related Infection. *Peptides 27*, 2104−2110.
(47) Ghiselli, R., Giacometti, A., Cirioni, O., Mocchegiani, F., Silvestri, C., Orlando, F., Kamysz, W., Licci, A., Nadolski, P., Della Vittoria, A., Łukasiak, J., Scalise, G., and Saba, V. (2007) Pretreatment with the Protegrin IB-367 Affects Gram-Positive Biofilm and Enhances the Therapeutic Efficacy of Linezolid in Animal Models of Central Venous Catheter Infection. *JPEN, J. Parenter. Enteral Nutr. 31*, 463−468.
(48) Zmistowski, B., Karam, J. A., Durinka, J. B., Casper, D. S., and Parvizi, J. (2013) Periprosthetic Joint Infection Increases the Risk of One-Year Mortality. *J. Bone Joint Surg. Am. 95*, 2177−2184.
(49) Mandell, J. B., Deslouches, B., Montelaro, R. C., Shanks, R. M. Q., Doi, Y., and Urish, K. L. (2017) Elimination of Antibiotic Resistant Surgical Implant Biofilms Using an Engineered Cationic Amphipathic Peptide WLBU2. *Sci. Rep. 7*, 18098.
(50) Minardi, D., Ghiselli, R., Cirioni, O., Giacometti, A., Kamysz, W., Orlando, F., Silvestri, C., Parri, G., Kamysz, E., Scalise, G., Saba, V., and Giovanni, M. (2007) The Antimicrobial Peptide Tachyplesin III Coated Alone and in Combination with Intraperitoneal Piperacillin-Tazobactam Prevents Ureteral Stent Pseudomonas Infection in a Rat Subcutaneous Pouch Model. *Peptides 28*, 2293−2298.
(51) Chen, R., Willcox, M. D. P., Ho, K. K. K., Smyth, D., and Kumar, N. (2016) Antimicrobial Peptide Melimine Coating for Titanium and Its in vivo Antibacterial Activity in Rodent Subcutaneous Infection Models. *Biomaterials 85*, 142−151.
(52) Yu, Q., Deng, T., Lin, F.-C., Zhang, B., and Zink, J. I. (2020) Supramolecular Assemblies of Heterogeneous Mesoporous Silica Nanoparticles to Co-Deliver Antimicrobial Peptides and Antibiotics for Synergistic Eradication of Pathogenic Biofilms. *ACS Nano 14*, 5926−5937.
(53) Ma, L., Ye, X., Sun, P., Xu, P., Wang, L., Liu, Z., Huang, X., Bai, Z., and Zhou, C. (2020) Antimicrobial and Antibiofilm Activity of the EeCentrocin 1 Derived Peptide EC1−17KV via Membrane Disruption. *EBioMedicine 55*, 102775.
(54) Lee, J.-K., Mereuta, L., Luchian, T., and Park, Y. (2019) Antimicrobial Peptide HPA3NT3-A2 Effectively Inhibits Biofilm Formation in Mice Infected with Drug-Resistant Bacteria. *Biomater. Sci. 7*, 5068−5083.
(55) Narayana, J. L., Mishra, B., Lushnikova, T., Golla, R. M., and Wang, G. (2019) Modulation of Antimicrobial Potency of Human Cathelicidin Peptides against the ESKAPE Pathogens and *in vivo* Efficacy in a Murine Catheter-Associated Biofilm Model. *Biochim. Biophys. Acta, Biomembr. 1861*, 1592−1602.
(56) Balaban, N., Gov, Y., Giacometti, A., Cirioni, O., Ghiselli, R., Mocchegiani, F., Orlando, F., D'Amato, G., Saba, V., Scalise, G., Bernes, S., and Mor, A. (2004) A Chimeric Peptide Composed of a Dermaseptin Derivative and an RNA III-Inhibiting Peptide Prevents Graft-Associated Infections by Antibiotic-Resistant Staphylococci. *Antimicrob. Agents Chemother. 48*, 2544−2550.

https://dx.doi.org/10.1021/acsptsci.0c00191
ACS Pharmacol. Transl. Sci. 2021, 4, 55−73

(57) Ju, X., Chen, J., Zhou, M., Zhu, M., Li, Z., Gao, S., Ou, J., Xu, D., Wu, M., Jiang, S., Hu, Y., Tian, Y., and Niu, Z. (2020) Combating Pseudomonas Aeruginosa Biofilms by a Chitosan-PEG-Peptide Conjugate via Changes in Assembled Structure. *ACS Appl. Mater. Interfaces 12*, 13731−13738.
(58) Stefani, S., Campana, S., Cariani, L., Carnovale, V., Colombo, C., Lleo, M. M., Iula, V. D., Minicucci, L., Morelli, P., Pizzamiglio, G., and Taccetti, G. (2017) Relevance of Multidrug-Resistant *Pseudomonas aeruginosa* Infections in Cystic Fibrosis. *Int. J. Med. Microbiol. 307*, 353−362.
(59) Ciofu, O., Tolker-Nielsen, T., Jensen, P. Ø., Wang, H., and Høiby, N. (2015) Antimicrobial Resistance, Respiratory Tract Infections and Role of Biofilms in Lung Infections in Cystic Fibrosis Patients. *Adv. Drug Delivery Rev. 85*, 7−23.
(60) Zhang, L., Parente, J., Harris, S. M., Woods, D. E., Hancock, R. E. W., and Falla, T. J. (2005) Antimicrobial Peptide Therapeutics for Cystic Fibrosis. *Antimicrob. Agents Chemother. 49*, 2921−2927.
(61) Mardirossian, M., Pompilio, A., Crocetta, V., De Nicola, S., Guida, F., Degasperi, M., Gennaro, R., Di Bonaventura, G., and Scocchi, M. (2016) *In vitro* and *in vivo* Evaluation of BMAP-Derived Peptides for the Treatment of Cystic Fibrosis-Related Pulmonary Infections. *Amino Acids 48*, 2253−2260.
(62) Harrington, N. E., Sweeney, E., and Harrison, F. (2020) Building a Better Biofilm - Formation of *in vivo*-like Biofilm Structures by *Pseudomonas aeruginosa* in a Porcine Model of Cystic Fibrosis Lung Infection. *Biofilm 2*, 100024.
(63) Song, Z., Wu, H., Mygind, P., Raventos, D., Sonksen, C., Kristensen, H.-H., and Høiby, N. (2005) Effects of Intratracheal Administration of Novispirin G10 on a Rat Model of Mucoid *Pseudomonas aeruginosa* Lung Infection. *Antimicrob. Agents Chemother. 49*, 3868−3874.
(64) Bayes, H. K., Ritchie, N., Irvine, S., and Evans, T. J. A (2016) Murine Model of Early *Pseudomonas aeruginosa* Lung Disease with Transition to Chronic Infection. *Sci. Rep. 6*, 35838.
(65) Martínez, M., Polizzotto, A., Flores, N., Semorile, L., and Maffía, P. C. (2020) Antibacterial, Anti-Biofilm and *in vivo* Activities of the Antimicrobial Peptides P5 and P6.2. *Microb. Pathog. 139*, 103886.
(66) Mwangi, J., Yin, Y., Wang, G., Yang, M., Li, Y., Zhang, Z., and Lai, R. (2019) The Antimicrobial Peptide ZY4 Combats Multidrug-Resistant *Pseudomonas aeruginosa* and *Acinetobacter baumannii* Infection. *Proc. Natl. Acad. Sci. U. S. A. 116*, 26516−26522.
(67) Chen, C., Mangoni, M. L., and Di, Y. P. (2017) *In vivo* Therapeutic Efficacy of Frog Skin-Derived Peptides Against *Pseudomonas aeruginosa*-Induced Pulmonary Infection. *Sci. Rep. 7*, 8548.
(68) Di, Y. P., Lin, Q., Chen, C., Montelaro, R. C., Doi, Y., and Deslouches, B. (2020) Enhanced Therapeutic Index of an Antimicrobial Peptide in Mice by Increasing Safety and Activity against Multidrug-Resistant Bacteria. *Sci. Adv. 6*, eaay6817.
(69) Murphy, C. N., and Clegg, S. (2012) *Klebsiella pneumoniae* and Type 3 Fimbriae: Nosocomial Infection, Regulation and Biofilm Formation. *Future Microbiol. 7*, 991−1002.
(70) Nair, G. B., and Niederman, M. S. (2015) Ventilator-Associated Pneumonia: Present Understanding and Ongoing Debates. *Intensive Care Med. 41*, 34−48.
(71) Guilhen, C., Miquel, S., Charbonnel, N., Joseph, L., Carrier, G., Forestier, C., and Balestrino, D. (2019) Colonization and Immune Modulation Properties of *Klebsiella pneumoniae* Biofilm-Dispersed Cells. *npj Biofilms Microbiomes 5*, 25.
(72) Tan, S., Gan, C., Li, R., Ye, Y., Zhang, S., Wu, X., Yang, Y. Y., Fan, W., and Wu, M. (2015) A Novel Chemosynthetic Peptide with β-Sheet Motif Efficiently Kills *Klebsiella pneumoniae* in a Mouse Model. *Int. J. Nanomed. 10*, 1045−1059.
(73) Bowen, W. H., Burne, R. A., Wu, H., and Koo, H. (2018) Oral Biofilms: Pathogens, Matrix, and Polymicrobial Interactions in Microenvironments. *Trends Microbiol. 26*, 229−242.
(74) Zhang, T., Wang, Z., Hancock, R. E. W., de la Fuente-Núñez, C., and Haapasalo, M. (2016) Treatment of Oral Biofilms by a D-Enantiomeric Peptide. *PLoS One 11*, e0166997.
(75) Dashper, S. G., Liu, S. W., and Reynolds, E. C. (2007) Antimicrobial Peptides and Their Potential as Oral Therapeutic Agents. *Int. J. Pept. Res. Ther. 13*, 505−516.
(76) Kim, D., Liu, Y., Benhamou, R. I., Sanchez, H., Simón-Soro, Á., Li, Y., Hwang, G., Fridman, M., Andes, D. R., and Koo, H. (2018) Bacterial-Derived Exopolysaccharides Enhance Antifungal Drug Tolerance in a Cross-Kingdom Oral Biofilm. *ISME J. 12*, 1427−1442.
(77) Bowen, W. H. (2013) Rodent Model in Caries Research. *Odontology 101*, 9−14.
(78) Liang, J., Liang, D., Liang, Y., He, J., Zuo, S., and Zhao, W. (2021) Effects of a Derivative of Reutericin 6 and Gassericin A on the Biofilm of *Streptococcus mutans in vitro* and Caries Prevention *in vivo*. *Odontology 109*, 53.
(79) Wang, Y., Wang, X., Jiang, W., Wang, K., Luo, J., Li, W., Zhou, X., and Zhang, L. (2018) Antimicrobial Peptide GH12 Suppresses Cariogenic Virulence Factors of *Streptococcus mutans*. *J. Oral Microbiol. 10*, 1442089.
(80) Wang, Y., Fan, Y., Zhou, Z., Tu, H., Ren, Q., Wang, X., Ding, L., Zhou, X., and Zhang, L. (2017) *De novo* Synthetic Short Antimicrobial Peptides against Cariogenic Bacteria. *Arch. Oral Biol. 80*, 41−50.
(81) Tu, H., Fan, Y., Lv, X., Han, S., Zhou, X., and Zhang, L. (2016) Activity of Synthetic Antimicrobial Peptide GH12 against Oral Streptococci. *Caries Res. 50*, 48−61.
(82) Wang, Y., Zeng, Y., Wang, Y., Li, H., Yu, S., Jiang, W., Li, Y., and Zhang, L. (2019) Antimicrobial Peptide GH12 Targets *Streptococcus mutans* to Arrest Caries Development in Rats. *J. Oral Microbiol. 11*, 1549921.
(83) Jiang, W., Wang, Y., Luo, J., Chen, X., Zeng, Y., Li, X., Feng, Z., and Zhang, L. (2020) Antimicrobial Peptide GH12 Prevents Dental Caries by Regulating Dental Plaque Microbiota. *Appl. Environ. Microbiol. 86*, e00527.
(84) Daep, C. A., James, D. M., Lamont, R. J., and Demuth, D. R. (2006) Structural Characterization of Peptide-Mediated Inhibition of *Porphyromonas gingivalis* Biofilm Formation. *Infect. Immun. 74*, 5756−5762.
(85) Daep, C. A., Novak, E. A., Lamont, R. J., and Demuth, D. R. (2011) Structural Dissection and *in vivo* Effectiveness of a Peptide Inhibitor of *Porphyromonas gingivalis* Adherence to *Streptococcus gordonii*. *Infect. Immun. 79*, 67−74.
(86) Lamont, R. J., El-Sabaeny, A., Park, Y., Cook, G. S., Costerton, J. W., and Demuth, D. R. (2002) Role of the *Streptococcus gordonii* SspB Protein in the Development of *Porphyromonas gingivalis* Biofilms on Streptococcal Substrates. *Microbiology 148*, 1627−1636.
(87) Chopra, A., Bhat, S. G., and Sivaraman, K. (2020) *Porphyromonas gingivalis* Adopts Intricate and Unique Molecular Mechanisms to Survive and Persist within the Host: A Critical Update. *J. Oral Microbiol. 12*, 1801090.
(88) Baker, P. J., Dixon, M., and Roopenian, D. C. (2000) Genetic Control of Susceptibility to *Porphyromonas gingivalis*-Induced Alveolar Bone Loss in Mice. *Infect. Immun. 68*, 5864−5868.
(89) Mahmoud, M. Y., Steinbach-Rankins, J. M., and Demuth, D. R. (2019) Functional Assessment of Peptide-Modified PLGA Nanoparticles against Oral Biofilms in a Murine Model of Periodontitis. *J. Controlled Release 297*, 3−13.
(90) Yu, H.-Y., Tu, C. H., Yip, B.-S., Chen, H.-L., Cheng, H.-T., Huang, K.-C., Lo, H.-J., and Cheng, J. W. (2011) Easy Strategy to Increase Salt Resistance of Antimicrobial Peptides. *Antimicrob. Agents Chemother. 55*, 4918−4921.
(91) Wang, H.-Y., Cheng, J.-W., Yu, H.-Y., Lin, L., Chih, Y.-H., and Pan, Y.-P. (2015) Efficacy of a Novel Antimicrobial Peptide against Periodontal Pathogens in Both Planktonic and Polymicrobial Biofilm States. *Acta Biomater. 25*, 150−161.
(92) Wang, H., Lin, L., Fu, W., Yu, H.-Y., Yu, N., Tan, L., Cheng, J., and Pan, Y. (2017) Preventive Effects of the Novel Antimicrobial Peptide Nal-P-113 in a Rat Periodontitis Model by Limiting the Growth of *Porphyromonas gingivalis* and Modulating IL-1β and TNF-α Production. *BMC Complementary Altern. Med. 17*, 426.
(93) Wang, H., Ai, L., Zhang, Y., Cheng, J., Yu, H., Li, C., Zhang, D., Pan, Y., and Lin, L. (2018) The Effects of Antimicrobial Peptide Nal-P-

113 on Inhibiting Periodontal Pathogens and Improving Periodontal Status. *BioMed Res. Int. 17*, 1805793.
(94) Denayer, T., Stöhr, T., and Van Roy, M. (2017) Animal Models in Translational Medicine: Validation and Prediction. *New Horiz. Transl. Med. 2*, 5−11.
(95) Rumbaugh, K. P. (2020) How Well Are We Translating Biofilm Research from Bench-Side to Bedside? *Biofilm 2*, 100028.
(96) Mercer, D. K., Torres, M. D. T., Duay, S. S., Lovie, E., Simpson, L., von Köckritz-Blickwede, M., de la Fuente-Nunez, C., O'Neil, D. A., and Angeles-Boza, A. M. (2020) Antimicrobial Susceptibility Testing of Antimicrobial Peptides to Better Predict Efficacy. *Front. Cell. Infect. Microbiol. 10*, 326.
(97) Ogunniyi, A. D., Kopecki, Z., Hickey, E. E., Khazandi, M., Peel, E., Belov, K., Boileau, A., Garg, S., Venter, H., Chan, W. Y., Hill, P. B., Page, S. W., Cowin, A. J., and Trott, D. J. (2018) Bioluminescent Murine Models of Bacterial Sepsis and Scald Wound Infections for Antimicrobial Efficacy Testing. *PLoS One 13*, e0200195.
(98) Sheppard, W. L., Mosich, G. M., Smith, R. A., Hamad, C. D., Park, H. Y., Zoller, S. D., Trikha, R., McCoy, T. K., Borthwell, R., Hoang, J., Truong, N., Cevallos, N., Clarkson, S., Hori, K. R., van Dijl, J. M., Francis, K. P., Petrigliano, F. A., and Bernthal, N. M. (2020) Novel *in vivo* Mouse Model of Shoulder Implant Infection. J. *Shoulder and Elbow Surg. 29*, 1412−1424.
(99) Allesen-Holm, M., Barken, K. B., Yang, L., Klausen, M., Webb, J. S., Kjelleberg, S., Molin, S., Givskov, M., and Tolker-Nielsen, T. A. (2006) Characterization of DNA Release in *Pseudomonas aeruginosa* Cultures and Biofilms. *Mol. Microbiol. 59*, 1114−1128.
(100) Jung, C.-J., Hsu, R.-B., Shun, C.-T., Hsu, C.-C., and Chia, J.-S. (2017) AtlA Mediates Extracellular DNA Release, Which Contributes to *Streptococcus mutans* Biofilm Formation in an Experimental Rat Model of Infective Endocarditis. *Infect. Immun. 85*, e00252.
(101) Conover, M. S., Mishra, M., and Deora, R. (2011) Extracellular DNA Is Essential for Maintaining Bordetella Biofilm Integrity on Abiotic Surfaces and in the Upper Respiratory Tract of Mice. *PLoS One 6*, e16861.
(102) Alhede, M., Alhede, M., Qvortrup, K., Kragh, K. N., Jensen, P. Ø., Stewart, P. S., and Bjarnsholt, T. (2020) The origin of extracellular DNA in bacterial biofilm infections. *Pathog. Dis. 78*, ftaa018.
(103) Ponce-Angulo, D. G., Bautista-Hernández, L. A., Calvillo-Medina, R. P., Castro-Tecorral, F. I., Aparicio-Ozores, G., López-Villegas, E. O., Ribas-Aparicio, R. M., and Bautista-de Lucio, V. M. (2020) Microscopic Characterization of Biofilm in Mixed Keratitis in a Novel Murine Model. *Microb. Pathog. 140*, 103953.
(104) Doke, S. K., and Dhawale, S. C. (2015) Alternatives to Animal Testing: A Review. *Saudi Pharm. J. 23*, 223−229.

https://dx.doi.org/10.1021/acsptsci.0c00191
ACS Pharmacol. Transl. Sci. 2021, 4, 55−73